CLASSICAL BUCKLING OF CYLINDRICAL PANELS

By

JACK WILLIAM VETTER

Bachelor of Science
University of Kansas
Lawrence, Kansas
March, 1961

Master of Science
University of Kansas
Lawrence, Kansas
June, 1966

Submitted to the Faculty of the
Graduate College of the
Oklahoma State University
in partial fulfillment of
the requirements for
the Degree of
DOCTOR OF PHILOSOPHY
May, 1970

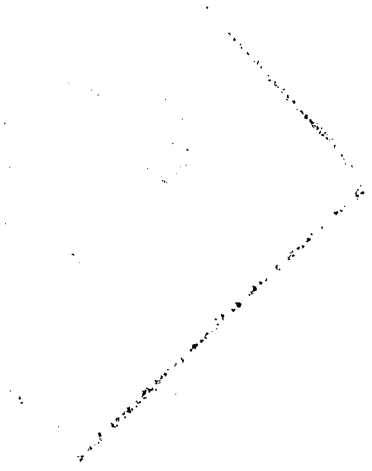

CLASSICAL BUCKLING OF

CYLINDRICAL PANELS

Thesis Approved:

Donald E. Boyd
Thesis Adviser

Ladislaus J. Fila

William P. Dawkins

D. Durham
Dean of the Graduate College

PREFACE

This work presents a numerical method to calculate the buckling modes for cylindrical panels which are simply supported along the curved edges. Trigonometric-power series displacement expressions are substituted into partial differential equations similar to Donnell's stability equations for circular cylinders. Consideration of a variable radius of curvature, expressed in terms of a power series in the transverse coordinate, is the additional feature of the equations. Use of the mixed-series displacement expressions allows treatment of a variable radius of curvature and also of any boundary conditions along the straight edges of the panel. This method is presented as a tool useful in estimating the buckling resistance for non-circular panels, which are common in some types of structures today.

I would like to express my sincere gratitude to the many who have helped make this work possible:

To Professor Donald E. Boyd, for his guidance and encouragement throughout my doctoral candidate studies and during preparation of this work;

To Professors Ahmed E. Salama, Ladislaus J. Fila, Philip N. Eldred, and W. P. Dawkins, for their interest and

advice while serving on the writer's advisory committee;

To Mr. Eldon J. Hardy for his friendship and for preparation of the drawings;

To Mrs. Carl Estes, who typed the manuscript;

Also, gratitude is expressed to the School of Civil Engineering at Oklahoma State University for its financial support during the writer's graduate studies.

TABLE OF CONTENTS

LIST OF TABLES

LIST OF FIGURES

NOMENCLATURE

a	Radius of circular shell
a_i	Coefficient in series describing curvature
D	Plate bending rigidity, $Eh^3/12(1-\nu^2)$
E	Young's modulus of elasticity
e	Classical strain
F	Body force per unit volume
G	Shearing modulus of elasticity
h	Shell wall thickness
i, j	Indices of summations
K	In-plane stiffness, $Eh/(1-\nu^2)$
k	Total number of terms taken in curvature series expression; twist or rotation gradient
L	Axial length
ℓ	Transverse panel width
Ms	Moment resultant acting on face perpendicular to s-direction
m	Number of longitudinal half waves
Ns	Normal force resultant acting on face perpendicular to s-direction
n	Index for displacement series
P	Maximum value taken for n
Q	Shearing force resultant
r	Local value of radius of curvature

s, x, z	Orthogonal coordinate axes
T	Temperature
t	Number of transverse half waves
V_i, U_i, W_i	Displacement series coefficients
v, u, w	Orthogonal displacement components
U	Strain energy
V	External potential
α_m	$m\pi\ell/L$
γ	Shearing strain
ϵ	Normal strain
η	Nondimensional longitudinal coordinate
λ	Scalar quantity
ν	Poisson's ratio
ξ	Nondimensional transverse coordinate; noncircularity parameter
ρ	Nondimensional radius of curvature
σ	Normal stress
τ	Shearing stress
ω	Rotation

CHAPTER I

INTRODUCTION

1.1 Statement of the Problem

The study of buckling of structures has been of practical importance for decades and especially so for modern aerospace, submarine, and similar metal structures. Recently, the more realistic cases involving large-deflections, creep, dynamic effects, initial imperfections, and so forth, have been emphasized in research (1). However, some interesting cases remain to be treated with the classical theoretical assumptions such as small deflections, undeformable normals, plane stress in the thin shell wall, and Hookean material. Moreover, the simple theory is a guide or starting point for more elaborate work. Classical buckling of cylindrical panels is a worthwhile field to investigate since panel members are used in aircraft, ships, and other stiffened structures. Recent works by Batdorf (2), Chu and Krishnamoorthy (3), Singer, Meer and Baruch (4), and many others, have investigated circular cylindrical panels under various loadings and with several boundary conditions. The basis for these works was the Donnell shell equations first set forth in 1933 (5).

These famous equations proved to be a useful simplification in shell theory and a concise discussion of their applicability appears in Kraus (6), pages 221-229.

Noncircular cylindrical shells and panels are an obviously more general case to be studied, especially since they are a common structure component. Marguerre first published a buckling paper in this field in 1942 (7) in which he analyzed open noncircular shells, simply supported along the longitudinal edges and subjected to torsion and compression. Marguerre proposed, in regard to buckling, to "regard minimum curvature alone as decisive," a key point. This work set the pattern for Kemper and Romano (8), who analyzed a noncircular shell under lateral pressure for stresses, and also for the present work.

This study presents a general method to analyze the classical buckling behavior of cylindrical panels which are simply supported along the curved edges. The boundary conditions are arbitrary along the straight edges and the radius of curvature may vary in the transverse (or circumferential) direction. The method also can be applied to closed shells with appropriate conditions of symmetry so that a segment of the closed shell might be analyzed as an open shell, or panel. The basic differential equations used are analogous to Donnell's shell equations. The method was verified by comparisons with the results of other investigators.

1.2 Solution Approach

The typical panel, along with the sign conventions, is shown in Figures 1 through 4. The local coordinate system is composed of the s, x, and z axes, which provide the transverse, longitudinal, and normal coordinates, respectively. The corresponding displacements are denoted by v, u, and w. The rotation components are ω_s and ω_x. The local value of the radius of curvature is denoted by r and the shell thickness is h. The normal and shearing stresses, and the normal force, shearing force, bending moment, and twisting moment resultants follow conventional notation (9).

Marguerre (7) expressed the panel curvature in terms of a trigonometric polynomial function of the transverse coordinate. Marguerre also indicated how to derive the cross section, given the curvature expression. Like Kemper (8 and 9), the present study will employ a simple version of this expression, consisting of a constant plus a sinusoidally varying term:

$$\frac{1}{r} = \frac{1}{a}\left(1 - \xi \cos \frac{2s}{a}\right) . \qquad (1.1)$$

In the preceding expression, a is the average radius for a closed noncircular cylinder and ξ is a constant defining the degree of noncircularity. The ξ parameter can take values from zero to one. The zero value corresponds to the circular cylinder and the value of one produces zero curvature at points along the cylinder circumference.

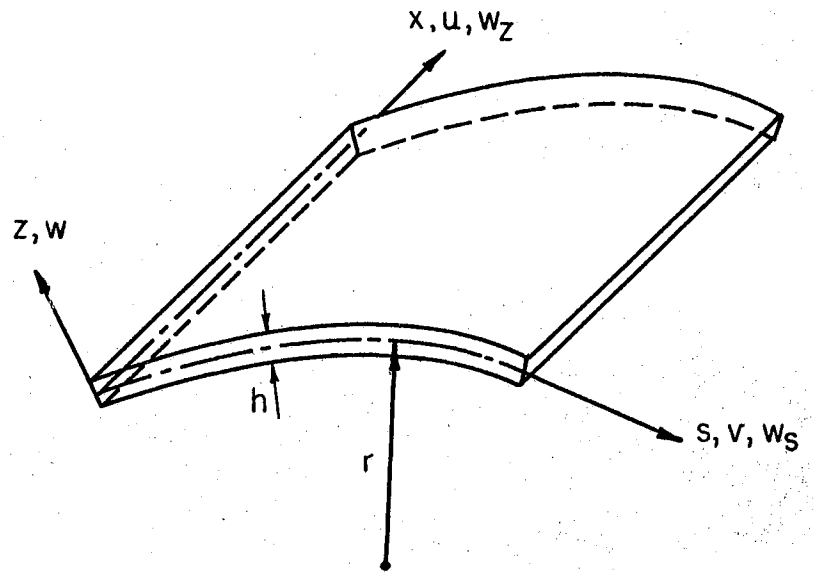

Figure 1. Shell Coordinate Axes, Displacement and Rotation Components

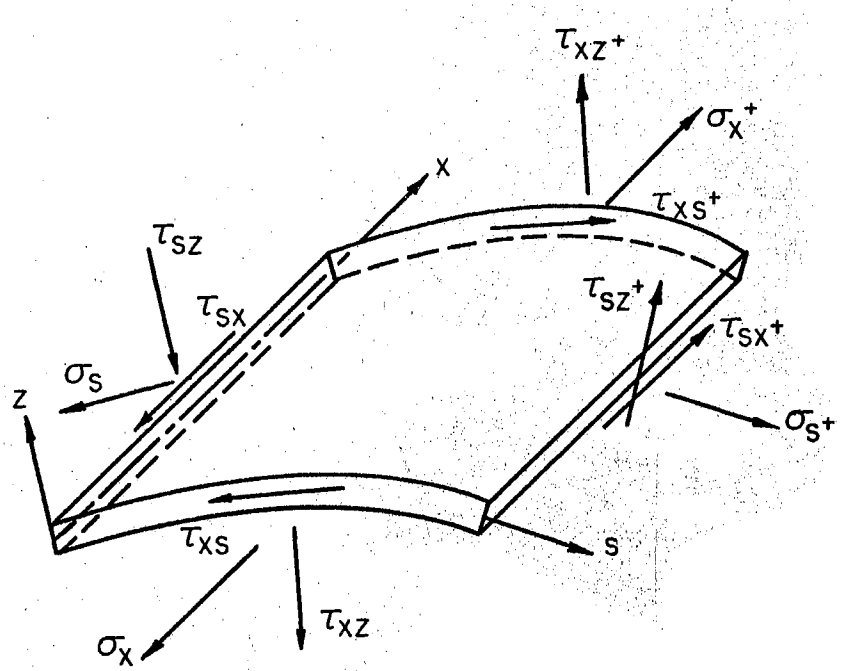

Figure 2. Stress Sign Convention

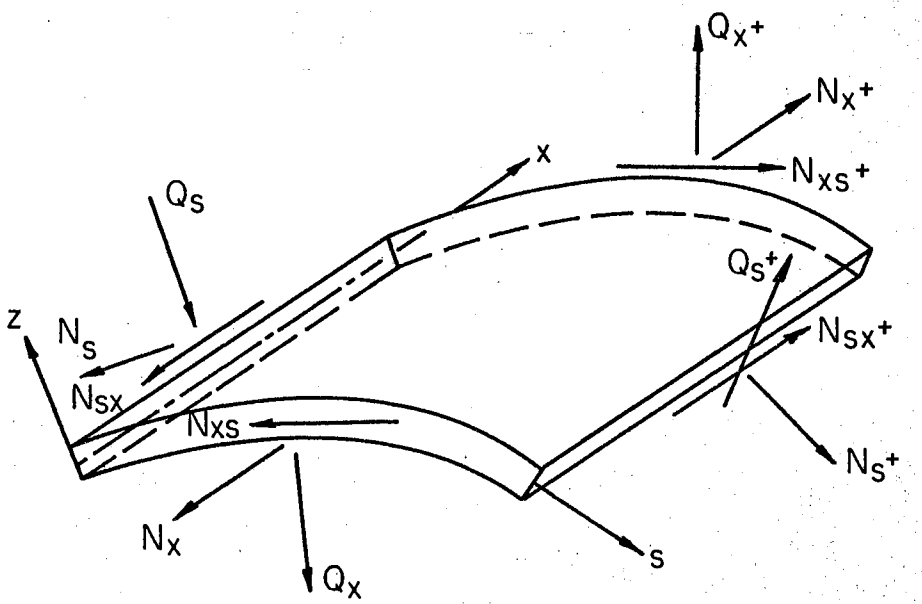

Figure 3. Force Resultant Sign Convention

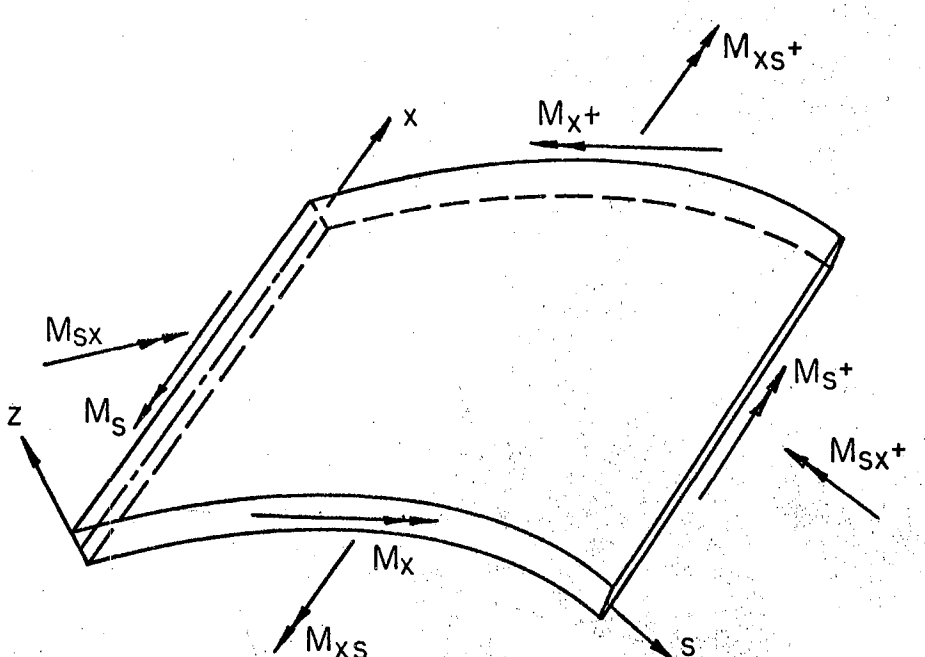

Figure 4. Moment Resultant Sign Convention

The basic equations used herein are analogous to the uncoupled Donnell shell equations. The solution approach follows that of Boyd (11) in that a mixed-series set of displacement expressions is employed, trigonometric series in the longitudinal direction and power series in the transverse direction. To agree with the approach, the curvature expression is also written explicitly as a power series. The displacement expressions will be found to satisfy simply supported conditions along the curved edges of the panel, while the boundary conditions are not specified along the straight edges by these expressions.

When the displacement and curvature expressions are substituted into the basic equations, a set of recurrence relations among the displacement series coefficients results. The expressions for the boundary conditions along the straight edges are joined with the above-mentioned recurrence relations to provide enough information to solve the problem for the unknown buckling loadings, and for the values of the displacement coefficients, or more precisely, the modal shapes. An advantage of the present method is that the boundary conditions are initially arbitrary along the straight edges and solutions for various sets may be investigated with little theoretical or practical difficulty. Also, more exact basic equations may be used with no particular difficuly.

CHAPTER II

FORMULATION OF THE BASIC RELATIONS

2.1 Derivation of Recurrence Relations Among the Displacement Series Coefficients

The basic equations employed in this study are analogous to Donnell's equations for buckling resulting from lateral pressure and axial compression. They are applied to thin cylindrical panels of constant thickness and uniform temperature, made of isotropic Hookean material. Assumptions are the Kirchhoff-Love hypotheses of nondeformable normals, plane stress in the panel wall, and small deflections. The basic equations are one result of a derivation based on energy methods that is presented in Appendix A. For completeness, both equilibrium and stability equations, and associated boundary conditions, for cylindrical shells are presented there.

The stability equations may be written in terms of the displacements caused by buckling, v, u, and w by using the force- and moment-resultant strain relationships:

$$u_{xx} + \frac{1+\nu}{2} v_{xs} + \frac{1-\nu}{2} u_{ss} + \frac{\nu}{r} w_x = 0 \qquad (2.1)$$

$$v_{ss} + \frac{1+\nu}{2} u_{xs} + \frac{1-\nu}{2} v_{xx} + \left(\frac{w}{r}\right)_s = 0 \qquad (2.2)$$

$$\nabla^4 w + \frac{12}{rh^2} (v_s + \frac{w}{r} + \nu u_x) - \frac{1}{D}(N_x w_{xx} + N_s w_{ss}) = 0 \qquad (2.3)$$

where

s, x, z = transverse, longitudinal and radial coordinates, respectively

v, u, w = transverse, longitudinal and radial buckling displacements

$\nabla^4 = \frac{\partial^4}{\partial s^4} + 2\frac{\partial^4}{\partial s^2 \partial x^2} + \frac{\partial^4}{\partial x^4}$

r = local value of radius of curvature

h = shell thickness

ν = Poisson's ratio

D = flexural stiffness $= \frac{Eh^3}{12(1-\nu^2)}$

N_x = prebuckling force resultant resulting from axial load, positive for tension

N_s = prebuckling force resultant resulting from lateral pressure loading, positive for internal pressurization.

Since the curvature is to be expressed in terms of power series, the following mixed trigonometric-power series expressions describing the buckling displacements are chosen:

$$v = \sum_{m=1}^{\infty} \sum_{n=1}^{\infty} V_{mn} \xi^{(n-1)} \sin m\pi\eta$$

$$u = \sum_{m=1}^{\infty} \sum_{n=1}^{\infty} U_{mn} \xi^{(n-1)} \cos m\pi\eta \qquad (2.4)$$

$$w = \sum_{m=1}^{\infty} \sum_{n=1}^{\infty} W_{mn} \xi^{(n-1)} \sin m\pi\eta$$

where η is the nondimensional longitudinal coordinate

$$\eta = \frac{x}{L} \tag{2.5}$$

and ξ is the nondimensional transverse coordinate

$$\xi = \frac{s}{\ell} \tag{2.6}$$

and

L = longitudinal length

ℓ = transverse length of the middle surface

m = number of longitudinal half waves.

Inspection of equations (2.4) reveals that they satisfy simply supported boundary conditions along the edges where $\eta = 0$ or 1. The following nondimensional expression for curvature is adopted:

$$\frac{\ell}{r} = \sum_{i=1}^{k} a_i \, \xi^{(i-1)} \quad . \tag{2.7}$$

The displacement expressions equations (2.4) and the curvature expression equation (2.7) can now be substituted into the stability equations, (2.1, 2.2, 2.3). After some algebraic operations, the following equations are obtained:

$$\sum_{m=1}^{\infty} \sum_{n=1}^{\infty} \Bigg[- \frac{\ell}{L} m^2 \pi^2 U_{mn} \, \xi^{(n-1)} + \frac{1-\nu}{2} \cdot \frac{L}{\ell} (n-1)(n-2) U_{mn} \, \xi^{(n-3)} +$$

$$+ \frac{1+\nu}{2} m\pi (n-1) V_{mn} \, \xi^{(n-2)} +$$

$$+ \nu \sum_{i=1}^{k} a_i \, \xi^{(i-1)} m\pi \, W_{mn} \xi^{(n-1)} \Bigg] \sin m\pi\eta = 0 \tag{2.8}$$

$$\sum_{m=1}^{\infty}\sum_{n=1}^{\infty}\Bigg[\frac{(n-1)(n-2)}{\ell^2}\,V_{mn}\,\xi^{(n-3)} - \frac{1-\nu}{2}\cdot\frac{m^2\pi^2}{L^2}\,V_{mn}\,\xi^{(n-1)} -$$

$$- \frac{1+\nu}{2}(n-1)\,\frac{m\pi}{\ell L}\,U_{mn}\,\xi^{(n-2)} + \tag{2.9}$$

$$+ \frac{1}{\ell^2}\cdot\frac{\partial}{\partial\xi}\left(\sum_{i=1}^{k} a_i\,\xi^{(i-1)}\sum_{m=1}^{\infty}\sum_{n=1}^{\infty} W_{mn}\,\xi^{(n-1)}\right)\Bigg]\sin m\pi\eta = 0$$

$$\sum_{m=1}^{\infty}\sum_{n=1}^{\infty}\Bigg[\frac{m^4\pi^4}{L^4}\,W_{mn}\,\xi^{(n-1)} - 2\,\frac{m^2\pi^2}{L\ell}\,(n-1)(n-2)\,W_{mn}\,\xi^{(n-3)} +$$

$$+ (n-1)(n-2)(n-3)(n-4)\,W_{mn}\,\xi^{(n-5)} +$$

$$+ \frac{12}{\ell h^2}\sum_{i=1}^{k} a_i\,\xi^{(i-1)}\left(\frac{1}{\ell}\,(n-1)\,V_{mn}\,\xi^{(n-2)} - \nu\,\frac{m\pi}{L}\,U_{mn}\,\xi^{(n-1)} +\right.$$

$$\left. + \frac{1}{\ell}\sum_{j=1}^{k} a_j\,\xi^{(j-1)}\,W_{mn}\,\xi^{(n-1)}\right) + \frac{N_x m^2\pi^2}{DL^2}\,W_{mn}\,\xi^{(n-1)} -$$

$$- (n-1)(n-2)\,\frac{N_s}{D\ell^2}\,W_{mn}\,\xi^{(n-3)}\Bigg]\sin m\pi\eta = 0\ . \tag{2.10}$$

When the powers of ξ are adjusted to $(n-1)$ and account is taken of the linear independence of the terms of the double series, the following recurrence relations result among the unknown displacement coefficients:

$$- \alpha_m^{\,2}\,U_{mn} + \frac{1-\nu}{2}\,n(n+1)\,U_{m,n+2} + \frac{1+\nu}{2}\,\alpha_m n\,V_{m,n+1} +$$

$$+ \nu\,\alpha_m\sum_{i=1}^{k} a_i\,\delta_{n,i}\,W_{m,n-1+1} = 0 \tag{2.11}$$

$$n(n+1)\ V_{m,n+2} - \alpha_m{}^2\ \frac{1-\nu}{2}\ V_{mn} - \frac{1+\nu}{2}\ \alpha_m n\ U_{m,n+1} +$$

$$+ \sum_{i=1}^{k} a_i\ n\ \delta_{n,i-1}\ W_{m,n-i+2} = 0 \qquad (2.12)$$

$$\left(\alpha_m{}^2 + \frac{N_x \ell^2}{D}\right) \frac{\alpha_m{}^2}{N_4}\ W_{mn} - \left(n(n+1)\ \frac{N_s \ell^2}{D} + 2\ \frac{\alpha_m{}^2}{N_2}\right) W_{m,n+2} +$$

$$+ W_{m,n+4} + \frac{12\ell^2}{N_4 h^2}\left(\sum_{i=1}^{k} a_i (n-i+1)\delta_{n,i-1}\ V_{m,n-i+2} -\right.$$

$$- \nu\alpha_m \sum_{i=1}^{k} a_i\ \delta_{n,i}\ U_{m,n-i+1} +$$

$$\left. + \sum_{i=1}^{k}\sum_{j=1}^{k} a_i a_j\ \delta_{n,i+j-1}\ W_{m,n-i-j+2}\right) = 0 \qquad (2.13)$$

where

$$\alpha_m = \frac{m\pi\ell}{L}$$

$$\delta_{n,j} = \begin{cases} 0 & n < j \\ 1 & n \geq j \end{cases}$$

$$N_1 = (n+3)$$

$$N_2 = (n+3)(n+2)$$

$$N_3 = (n+3)(n+2)(n+1)$$

$$N_4 = (n+3)(n+2)(n+1)n\ .$$

In classical buckling problems, generally only one set of displacements exists for the minimum buckling load in any instance. Therefore, it is necessary to investigate a given shell or panel for different values of m and for various sets of transverse modal shapes in order to find the minimum buckling load. Choosing a value for m, there

remains a set of three recurrence relations among the infinite number of coefficients of the displacement series. It will be necessary to choose a maximum value for n (call it p) and so truncate the series as an approximation. Inspection of the recurrence relations indicates that the magnitudes of the coefficients should eventually decrease as n increases and evidently become negligible in their contribution to the displacements. The appropriate value for p must remain a matter of judgement.

2.2 Statement of Boundary Conditions

Inspection of the displacement expressions, equations (2-4), reveals that they satisfy the following boundary conditions along the curved edges of constant x (where $\eta = 0$ or 1):

$$\begin{aligned} v &= 0 \\ N_\eta &= K\left[u_\eta + \nu\left(v_\xi + \frac{w}{r}\right)\right] = 0 \\ w &= 0 \\ w_{\eta\eta} &= 0, \text{ where } K = \frac{Eh}{(1-\nu^2)} \quad . \end{aligned} \tag{2.14}$$

These represent the familiar case of the simply supported edge. One important advantage of the present method is that the boundary conditions are still arbitrary along the straight edges of constant s (where $\xi = 0$ or 1). The three types of boundary conditions along the straight edges which were considered in the present work are:

(1) Simply supported (SS3 in notation of Ref. 4):

$$N_s = 0: \sum_{m=1}^{\infty} \sum_{n=1}^{\infty} (nV_{m,n+1} - \nu\alpha_m U_{mn} + \sum_{i=1}^{k} a_i \delta_{n,i} W_{m,n-i+1}) \xi^{(n-1)} \cos m\pi\eta = 0 \tag{2.15}$$

$$u = 0: \sum_{m=1}^{\infty} \sum_{n=1}^{\infty} U_{mn} \xi^{(n-1)} \cos m\pi\eta = 0 \tag{2.16}$$

$$w = 0: \sum_{m=1}^{\infty} \sum_{n=1}^{\infty} W_{mn} \xi^{(n-1)} \sin m\pi\eta = 0 \tag{2.17}$$

$$M_s = 0: \sum_{m=1}^{\infty} \sum_{n=1}^{\infty} [n(n+1) W_{m,n+2} - \nu\alpha_m^2 W_{mn}] \xi^{(n-1)} \sin m\pi\eta = 0. \tag{2.18}$$

(2) Simply supported with motion restricted in the transverse direction (SS4 in the notation of Ref. 4):

Same as equations (2.16 - 2.18), except the first condition becomes

$$v = 0: \sum_{m=1}^{\infty} \sum_{n=1}^{\infty} V_{mn} \xi^{(n-1)} \sin m\pi\eta = 0 \quad . \tag{2.19}$$

(3) Free edges:

$$N_s = 0: \sum_{m=1}^{\infty} \sum_{n=1}^{\infty} [n V_{m,n+1} - \nu\alpha_m U_{mn} + \sum_{i=1}^{k} a_i \delta_{n,i} W_{n-i+1}] \xi^{(n-1)} \cos m\pi\eta = 0 \tag{2.20}$$

$$N_{sx} = 0: \sum_{m=1}^{\infty} \sum_{n=1}^{\infty} [\alpha_m V_{mn} + n U_{m,n+1}] \xi^{(n-1)} \sin m\pi\eta = 0 \tag{2.21}$$

$$\frac{\partial M_s}{\partial s} + 2 \frac{\partial M_{xs}}{\partial s} = 0: \sum_{m=1}^{\infty} \sum_{n=1}^{\infty} [n\alpha_m^2 (2-\nu) W_{m,n+1} - n(n+1)(n+2) W_{m,n+3}] \xi^{(n-1)} \sin m\pi\eta = 0 \tag{2.22}$$

$$M_s = 0: \sum_{m=1}^{\infty} \sum_{n=1}^{\infty} [n(n+1) W_{m,n+2} - \nu\alpha_m^2 W_{mn}] \xi^{(n-1)} \sin m\pi\eta = 0 \ . \tag{2.23}$$

Inspection of these conditions will show that they satisfy the fuller statements of the boundary conditions as given in Appendix A. Now the recurrence relations (equations (2.11 - 2.13)) and the boundary conditions are ready for approximate solutions for the buckling eigenvalues and for the corresponding displacement series coefficients, for a given value of m.

CHAPTER III

NUMERICAL SOLUTION OF THE BUCKLING DETERMINANT

Equations (2-11) to (2-13) represent sets of relations among the infinite number of unknown displacement series coefficients. Restricting attention to those values of $n \leq p$, the recurrence relations may be arrayed as $3p$ equations, three for each value of n. In so doing, the assumption is made that only the first $p + 2$ coefficients of the u and v displacement series and the first $p + 4$ coefficients of the w series are practically important.

Thus, the total number of unknown coefficients is $3p + 8$. The eight additional equations involving the unknown coefficients are provided by the boundary conditions along the straight edges, four conditions on each edge. The recurrence relations and eight boundary conditions are arrayed as shown in Figure 5, so as to produce a well-conditioned matrix. The terms governing the problem solution are those resulting from external axial compression and lateral pressure; the values of these which result in a zero value of the determinant are the eigenvalues. The modal shapes can be calculated for a given eigenvalue, though the amplitudes of the v, u, and w shapes remain

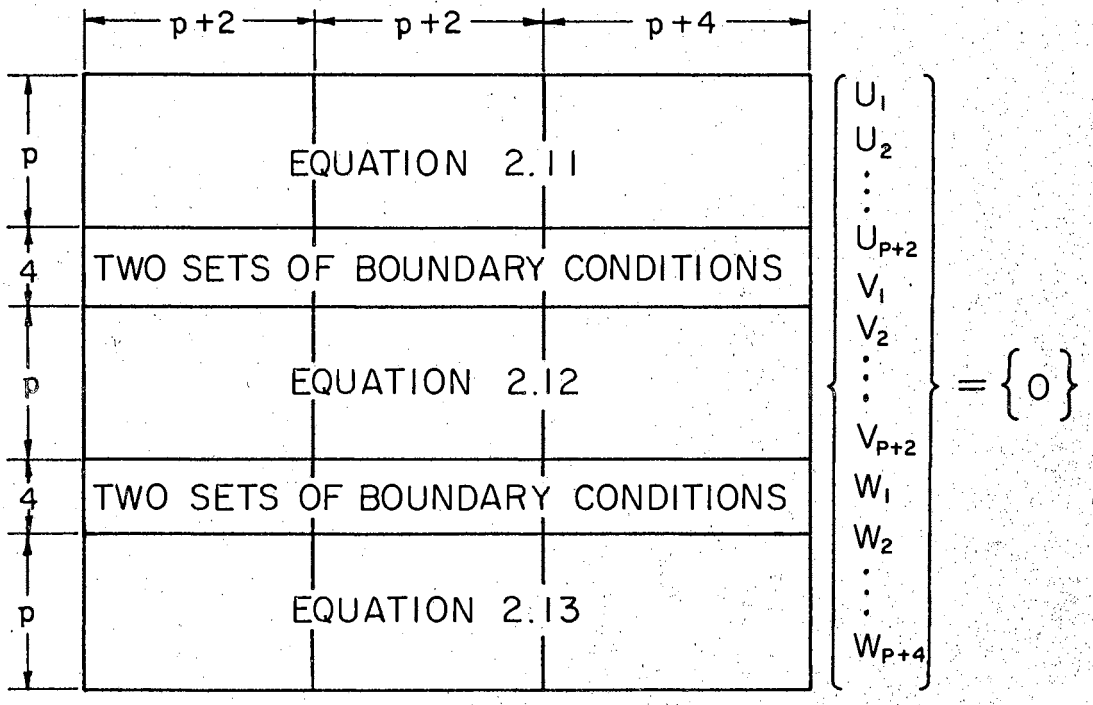

Figure 5. Schematic Drawing of Matrix of Equilibrium Equations and Boundary Conditions

indefinite, except in relation to each other. The symbol t will be used to denote the number of half waves in the transverse direction.

The calculations were carried out on an IBM model 360 computer in a straight-forward manner. Starting with a value close to the estimated eigenvalue, the determinant was calculated for incremental values until the sign changed. Then, Newton's method was used to converge as closely as desired to the eigenvalue. After the substitution of the final eigenvalue approximation into the set of recurrence relations, $3p + 7$ coefficients were determined in terms of the remaining coefficient, and the modal shapes in the transverse direction, corresponding to the eigenvalue, were plotted.

Owing to the chosen displacement expressions, equations (2.4), the modal shapes are sinusoidal in the longitudinal direction and the number of longitudinal half waves is determined by the chosen value of m. The modal shapes in the transverse direction may be difficult to categorize, for some boundary conditions, and sometimes the term "half wave" will be used in a rather loose way.

It may be noticed that the recurrence relations and boundary conditions, arranged as indicated in Figure 5, do not form the familiar eigenvalue matrix since the eigenvalue parameter does not appear in every term of the main diagonal. For this reason it is not possible to use an eigenvalue subroutine, which would save computation time.

It does not seem feasible to use the eighth order form of Donnell's equation, written in terms of w only, in order to reduce the problem and perhaps allow use of a standard eigenvalue subroutine, except in the case of simply supported boundary conditions along the straight edges (cf. Ref. 2). However, with the present form of three coupled equations in v, u, and w, changing the boundary conditions is a matter of exchanging a few cards in the computer program. Furthermore, the problem of encountering possible extraneous solutions to the eighth order equation is avoided (12).

CHAPTER IV

NUMERICAL RESULTS

4.1 Comparisons with Known Solutions

4.1.1 Introduction

It was decided to substantiate the general method of solution described in the previous chapters by comparison with the results of others, and to present examples of new problems which may be readily solved. Buckling solutions were found for the cases of axial loading, of lateral pressure loading, and for combination of the two, for circular and for noncircular shells, with various sets of boundary conditions.

4.1.2 Axially Loaded Circular Panels

The first case considered was the circular cylindrical panel under axial compressive loading and the results are given graphically in Figure 6. The central angle was 30 degrees and the aspect ratio was one to four, with the longer dimension along the straight edges. In this case, as in many others, the panel geometry was chosen to approximate realistic proportions, but at the same time, to be advantageous in keeping the number of terms required in the

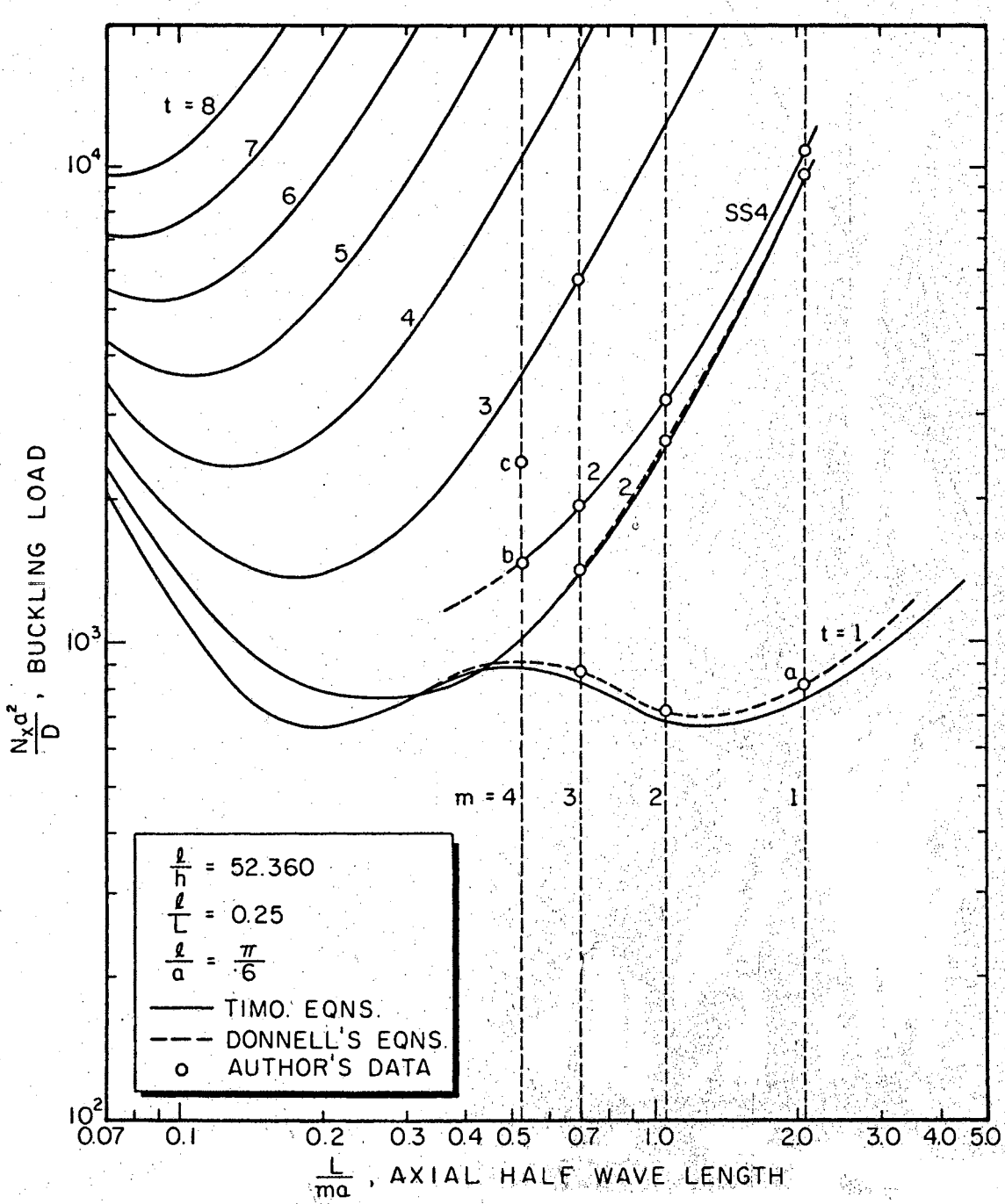

Figure 6. Buckling Load Parameter Versus Axial Half Wave Length Ratio for Axially Compressed Circular Panels with Simply Supported Straight Edges

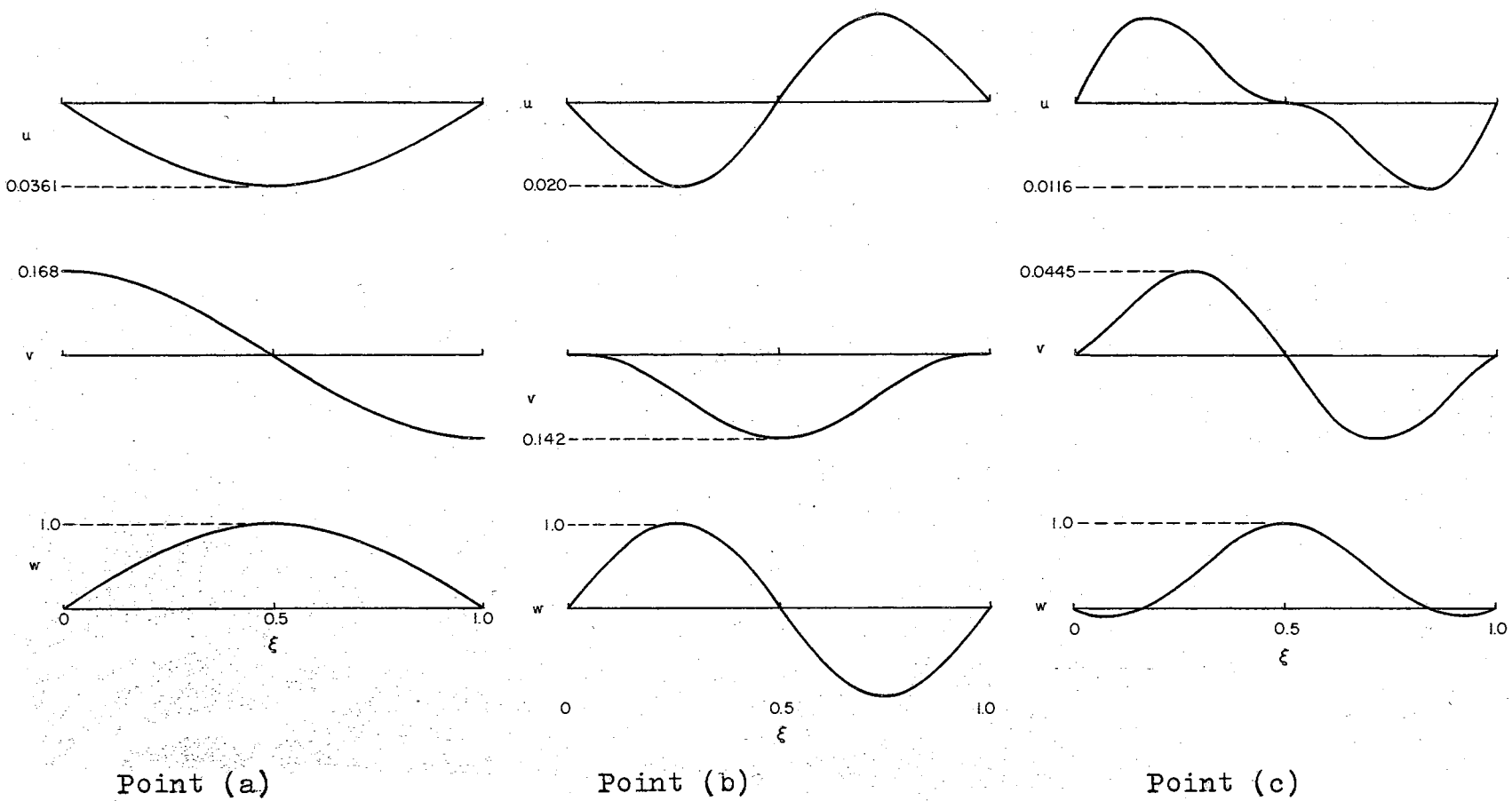

Figure 7. Relative u, v, and w Displacements Versus Transverse Coordinate ξ for Points a, b, and c, Figure 6

displacement functions relatively few, thereby keeping computation time short.

Referring to Figure 6, the buckling stress parameter, $N_x a^2/D$, is plotted versus the nondimensionalized axial half wave length ratio, L/ma, where m is the number of axial half waves and a is the radius. The various curves correspond to the numbers of circumferential half waves, denoted by t. The solid curves correspond to the solution of the buckling equations presented by Timoshenko (13) and the dotted lines represent those solutions of the corresponding Donnell's buckling equations which differ markedly from the former. Both sets of equations were solved by the substitution of double trigonometric series.

The author's data points agree with the results obtained by the substitution of double trigonometric series into Donnell's buckling equations. Typical modal shapes are shown in Figure 7, as calculated for pt. a. As could be expected, the maximum relative magnitude is greatest for the normal, or w, deflections. The maximum transverse and axial deflection amplitudes are successively less by roughly an order of magnitude, each. Note that, according to the deflection expressions, equations (2.4), the u displacement for m = 1 is greatest at either curved edge and zero in the center of the panel, lengthwise, and vice versa for the v and w displacements. The curves appear to be nicely sinusoidal.

Table I contains a comparison of some numerical results

TABLE I

COMPARISON WITH THE RESULTS OF TIMOSHENKO FOR AN AXIALLY COMPRESSED SIMPLY SUPPORTED CIRCULAR CYLINDRICAL PANEL

m =	t =	$\frac{N_{xa}^2}{D}$ Donnell	$\frac{N_{xa}^2}{D}$ Author	
1	1	820.297	820.174	$\frac{\ell}{h} = 52.35987$
1	2	9517.851	9535.930	$\frac{\ell}{L} = 0.25$
2	1	716.651	716.489	
2	2	2643.509	2647.723	$\frac{\ell}{a} = \frac{\ell}{r_o} = 0.5235987$
3	1	864.032	863.733	
3	2	1415.256	1415.243	
3	3	5871.128	5740.789	ν(Poisson's Ratio) = 0.28
4	1			

for points in Figure 6 for the buckling load parameter obtained by the solution of Donnell's equations through the substitution of double trigonometric series and through the substitution of the author's mixed series. On the basis of the above results, it is assumed that the method presented herein will converge to the double trigonometric series answer as closely as desired, given enough computer time and storage capacity.

The curve labeled SS4 (following the notation of Singer et al. (4)) represents the results obtained by cancelling transverse motion on the simply supported straight edges. Enough points were obtained to establish a curve for lower values of m. As m increases, the computation time required increases, and for this reason the minimum buckling stress was not established. However, it seems reasonable to expect a minimum buckling stress greater than for the "classical" simply supported case. This would agree with the results of Rehfield and Hallauer (14). The modal shapes for pt. b of Figure 6 are shown in Figure 7. As can be seen from the shapes, no additional circumferential membrane stress along the straight edges is generated by the buckling displacements. Point c of Figure 6 represents a point from some other curve of the SS4 case and the modal shapes are shown in Figure 7.

The next case considered was the axially compressed circular cylindrical panel with free edges as presented by Chu and Krishnamoorthy (3). These authors used the

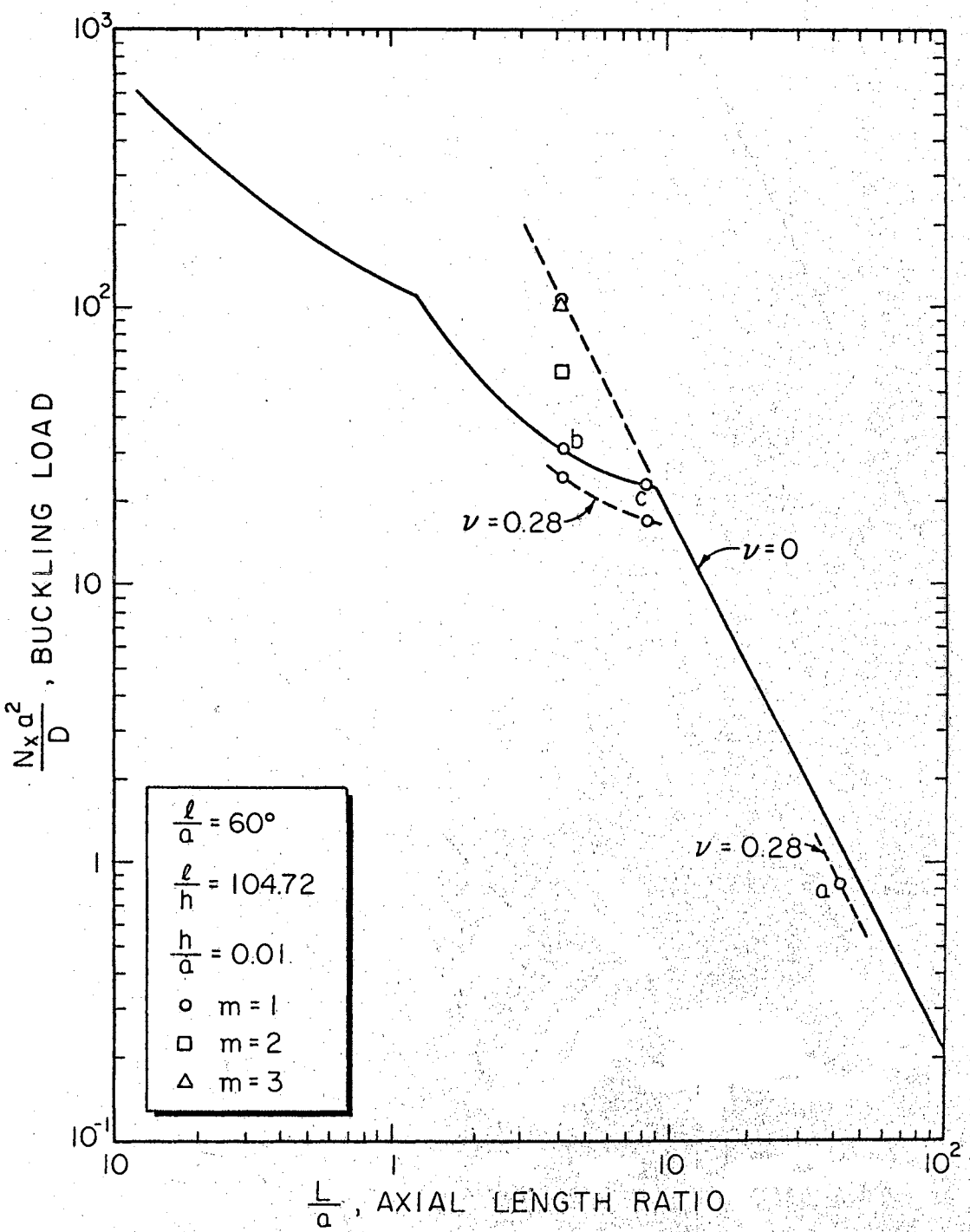

Figure 8. Buckling Load Parameter Versus Axial Length Ratio for the Axially Compressed Circular Panel with Free Straight Edges

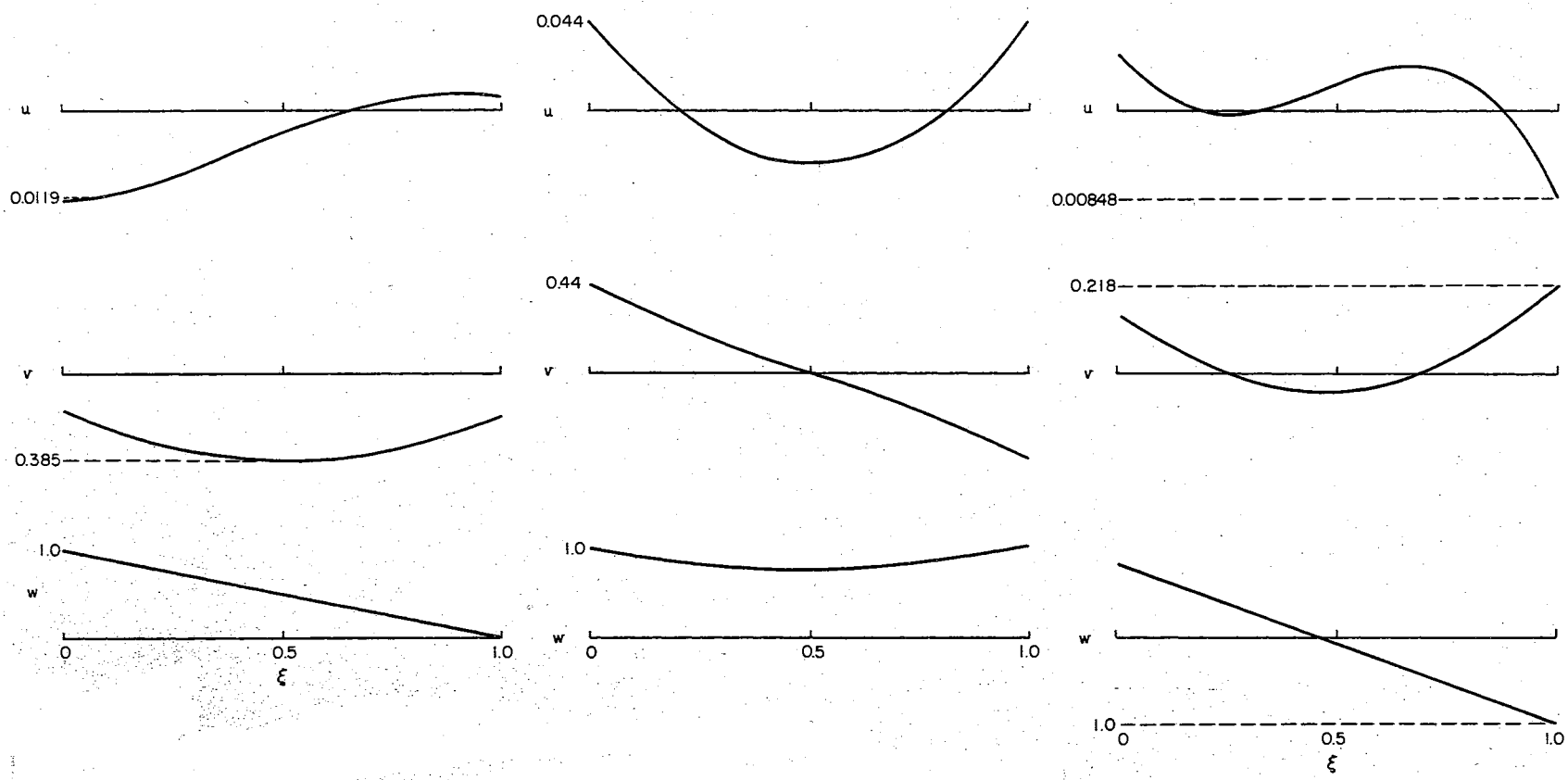

Point (a) Point (b) Point (c)

Figure 9. Relative u, v, and w Displacements Versus Transverse Coordinate ξ for Points a, b, and c, Figure 8

escalated form of Donnell's shell equations, with ν, Poisson's ratio equal to zero, and their results are shown in Figure 8. In this case, the panel central angle was 60° and the thickness was equal to 0.01 times the radius. Point a and two other points were found as buckling loads for the case with Poisson's ratio equal to 0.28, in order to study the importance of this factor. The effect is rather small, on the order of 10 to 15 percent. According to Chu and Krishnamoorthy, the minimum buckling load occurs for $m = 1$ and this was verified for pt. b by obtaining solutions for $m = 1$, 2, and 3.

The modal shapes for pts. a, b, and c are illustrated in Figure 9. It would seem to be difficult to make general descriptions of the modal shapes for this free-free case.

4.1.3 Circular Panels Under Normal Pressure

The next case considered was the circular cylindrical panel under lateral pressure loading, as first presented by Singer, Meer, and Baruch (4). Their Figure 2 is redrawn here as Figure 10, and the present author's data points are indicated as open circles. Agreement is generally good. It would be interesting to establish the reason for the differences to be noted on the lower curve, for simply supported boundary conditions along the straight edges. Probably these are due to an insufficient number of iterations or displacement series terms, but possibly differences might enter through another manner. The upper

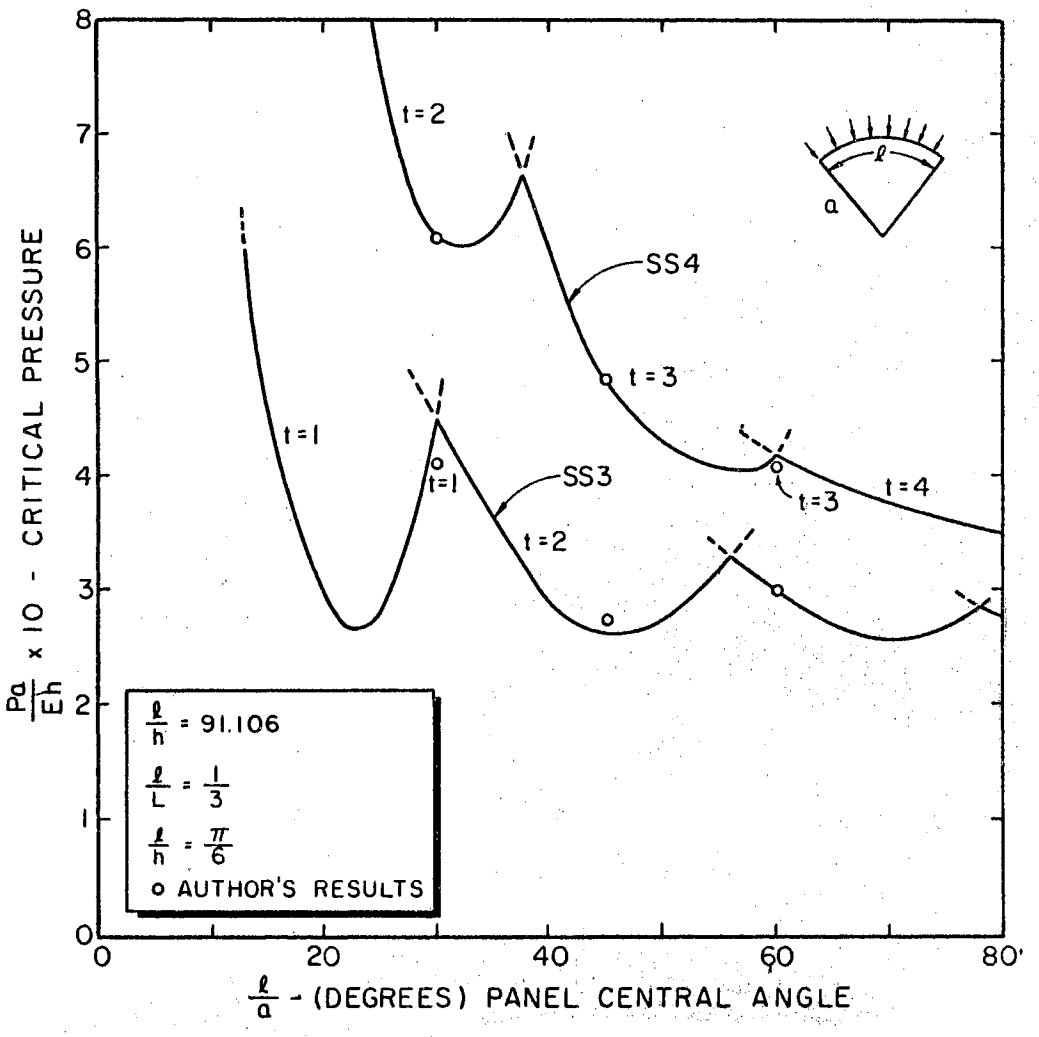

Figure 10. Critical Pressure Parameter Versus Circular Panel Central Angle for Two Sets of Boundary Conditions

curve was calculated by using the three coupled Donnell equations, whereas the lower curve was calculated by using the escalated eighth order form and it has been reported by Batdorf (12) that errors may arise from this process.

4.1.4 Oval Cylinders Under Axial Compression

The above cases were judged sufficient to prove the numerical method in regard to circular cylindrical panels. The next case considered was the oval cylindrical panel. To be more exact, the panel considered was one-fourth a closed oval shell studied by Kempner and Chen (10) for buckling and for postbuckling. Kempner and Chen described the curvature as follows:

$$\frac{1}{r} = \frac{1}{a}\left(1 - \xi \cos \frac{2s}{a}\right) \tag{4.1}$$

where a is the radius of a circular shell having the same perimeter as the oval shell in question and ξ is a constant with a value taken in the range from zero to one, where $\xi = 0$ corresponds to the circular cylindrical shell. The author calculated buckling solutions for $\xi = 0.1$ and 0.5 for a segment included between a major and a minor axis, with boundary conditions as illustrated in Figure 11.

The buckling calculations of Kempner and Chen assumed symmetry of deflections about the semi-minor axes, and due to the limitations on computer time, the author assumed symmetry about both semi-minor and semi-major axes. This evidently introduced a restriction on the deflection

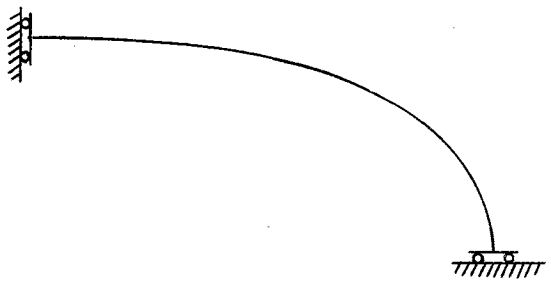

Figure 11. Segment of Non-circular Shell Considered as a Panel

configuration so that the buckling load was generally higher than the results of Kempner and Chen.

The results are shown in Figure 12. The ordinate represents buckling stress divided by the approximate buckling stress formula for the circular cylindrical shell:

$$\sigma_{cr}{}^{o} = \frac{Eh}{a} \cdot \frac{1}{\sqrt{3(1-\nu^2)}} \quad . \qquad (4.2)$$

The abscissa is the axial wave length parameter employed by Kempner and Chen: the axial full wave length divided by the perimeter. The curves labeled with n^* represent the buckling loads for circular cylindrical shells, corresponding to the Donnell equations, and n^* refers to the number of circumferential full waves. Two points were confirmed on these curves as a check.

The solid curves for nonzero ξ are the results of Kempner and Chen, for Donnell type equations, for the non-circular case, with odd numbers of transverse full waves. The author's results determined the broken line for $\xi = 0.1$.

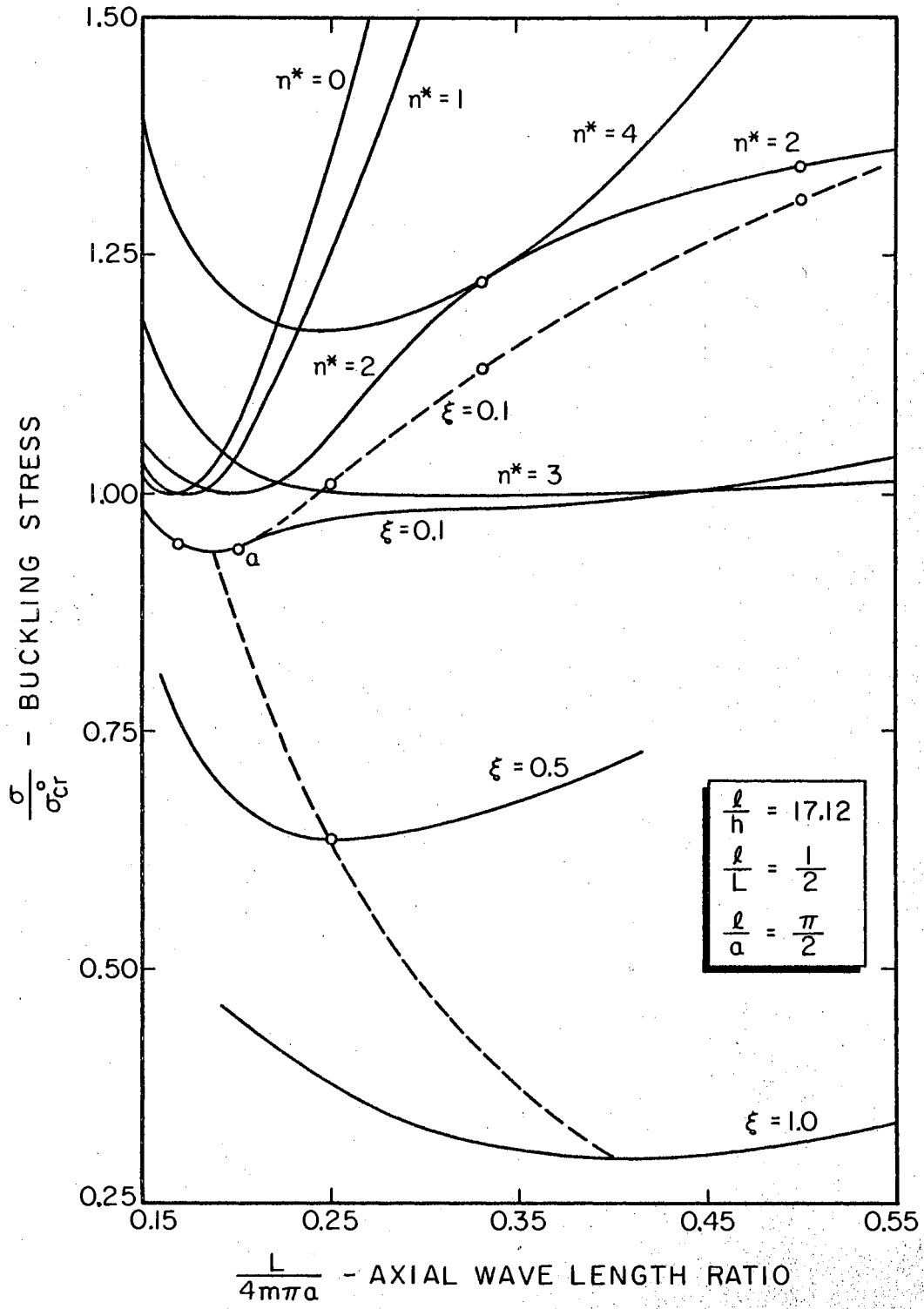

Figure 12. Buckling Load Parameter Versus Axial Wave Length Parameter for the Noncircular Cylinder

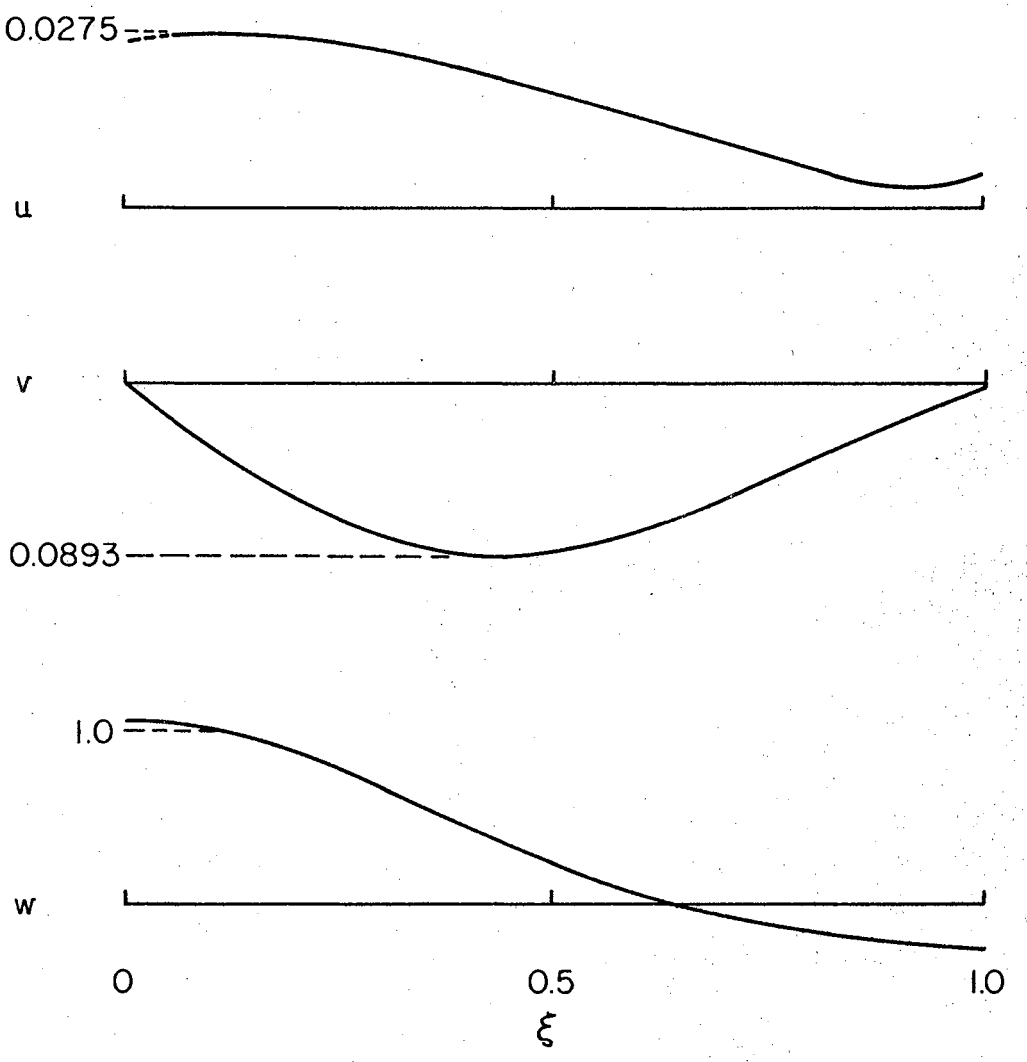

Figure 13. Relative u, v, and w Displacements Versus Transverse Coordinate Point a, Figure 12

This curve represents the buckling loads for the panel corresponding to a quarter section of the closed cylinder. The modal shapes for pt. a are shown in Figure 13. These indicate that $n^* = 2$ for the corresponding closed cylinder, and the shape of the dotted curve is similar to the case for $n^* = 2$ for the circular cylinder. The minimum buckling load seems to be equal to that of the curve of Kempner and Chen.

4.2 Study of Noncircular Cylindrical Panels

4.2.1 Combined Loading of Circular Cylindrical Panels

The next case studied was the circular cylindrical panel under combined axial compression and lateral pressure loading, with simply supported edges. The panel had a central angle of 45° and the aspect ratio of the transverse dimension, along the middle surface, to the axial dimension was one to four. The ratio of transverse length to thickness was 100 to 1. This problem is solved by Timoshenko (13), and Figure 14 represents a plot of solutions for the panel at hand. Nondimensionalized buckling parameters have been plotted. The substitition of double trigonometric series into the coupled Donnell's equations was used to form the buckling determinant to produce these results. Each solid line is numbered according to the number of longitudinal and transverse half

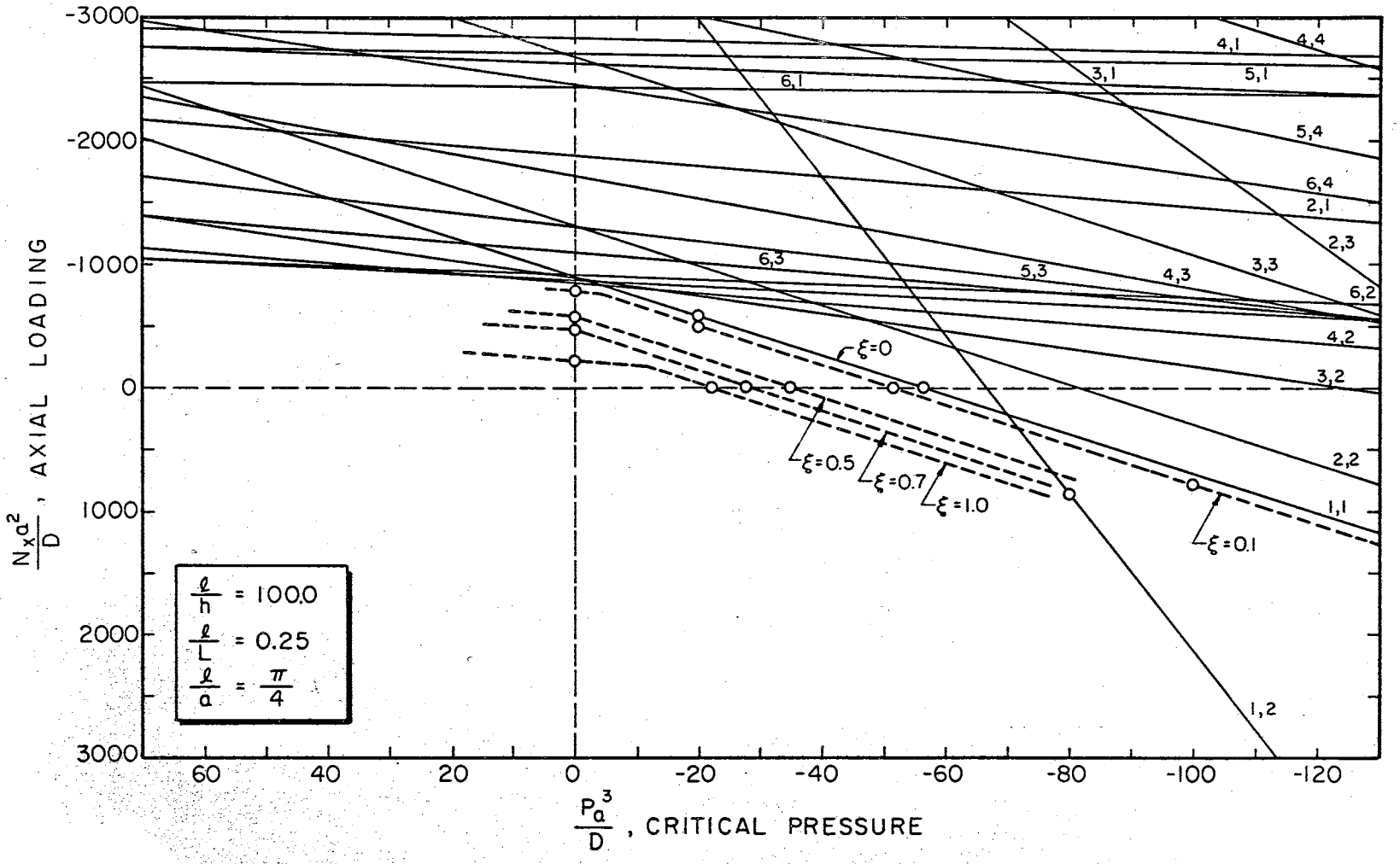

Figure 14. Combined Loading and the Effect of Noncircularity

waves of the w modal shape. Thus a straight line passing through the origin might be drawn to represent proportional loading and if the panel were loaded following this line, ideally it would pass through various buckled shapes corresponding to the lines traversed. Three points were confirmed very well by the computer program used herein.

4.2.2 Effect of Eccentricity Upon Buckling Loadings

Since the mixed-series method of solution presented here allows consideration of noncircularity and various boundary conditions, it was decided to study these effects on the load carrying capacity of the panel just described. For the sake of simplicity, the methods of loading were pure axial compression and pure lateral pressure. Equation (4.1) was chosen to describe the panel curvature. The values of ξ, the eccentricity parameter, studied were 0, .1, .5, .7, and 1. Of course, the value $\xi = 0$ corresponds to the circular panel and the symbol a represents the radius of this panel. Due to the form of equation (4.1), the radius of curvature varies in a sinusoidal manner, from an initial value, denoted by a_o, when $s = 0$, to the final value, a, at the other edge. The value of a_o depends upon the value of ξ but all the cases had the same value for a. (Actually these factors were handled nondimensional as ℓ/a_o and ℓ/a.)

The modal shape for the minimum buckling value of pure

axial compression loading with simply supported boundary conditions for the circular case shown in Figure 14 has m, the number of axial half waves, equal to 4 and n, the number of transverse half waves, equal to 2. For pure lateral pressure loading, in this case, the lowest critical pressure corresponds to $m = 1$ and $n = 1$. The buckling loading values for these cases, reduced by the effect of noncircularity, are indicated in Figure 14 and extrapolated broken lines indicate the probable buckling values for limited ranges of combined loading, for the values of ξ that were considered. The reduction in buckling loading with eccentricity is also shown in Figure 15.

As set forth by Marguerre (7), an approximate value for buckling loading may be calculated for a noncircular panel by basing the buckling calculation upon the minimum value for curvature, when the curvature varies along the breadth of the panel. This seems intuitively reasonable and is generally borne out by the results presented in Table II, in which the mixed-series results are compared with the approximations. The approximate answers are generally conservative and were calculated by using Donnell's equations to derive the buckling determinant. The nondimensional parameter used for the lateral pressure loading case did contain the maximum value for radius of curvature for noncircular panels and seems to be a useful arrangement of factors, since the approximate values are conservative. The approximate result for axial loading for $\xi = 1$ is nonconservative, however, and deserves further study.

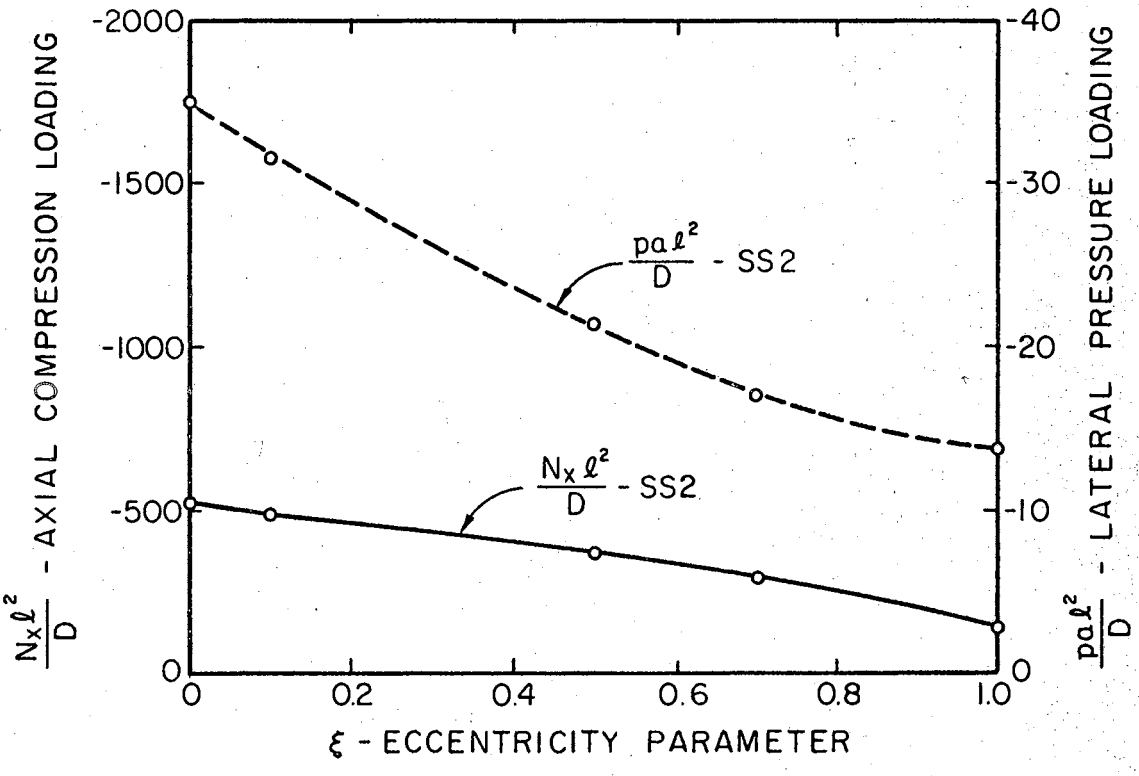

Figure 15. The Effect of Noncircularity Upon Buckling Loadings for Simply Supported Boundary Conditions

TABLE II

APPROXIMATE BUCKLING LOADING RESULTS FOR NON-CIRCULAR CYLINDRICAL PANELS

ξ	$\frac{\ell}{a_o}$	$\frac{N_x \ell^2}{D}$		$\frac{p a_o \ell^2}{D}$	
		circ.	noncirc.	circ.	noncirc.
0.0	0.78540	-520.	-524.	-34.8	-34.8
0.1	0.70686	-466.	-484.	-30.2	-31.7
0.5	0.39270	-315.	-355.	-17.0	-21.4
0.7	0.23562	-270.5	-292.	-13.3	-17.1
1.0	0.0	-246.	-136.	---	---

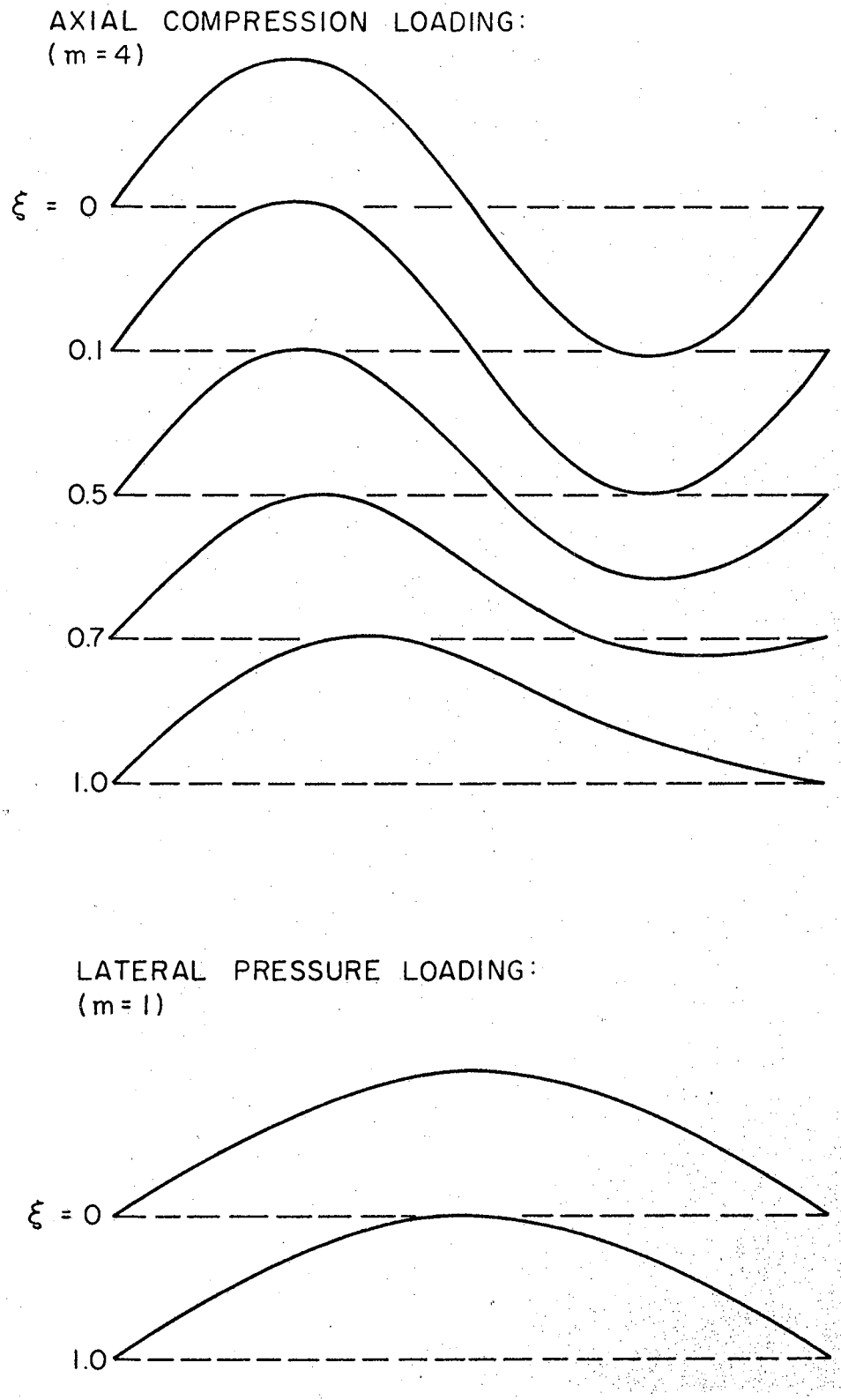

Figure 16. Normal (w) Deflection Modal Shapes for Axial Loading and for Lateral Pressure Loading, with Simply Supported Boundary Conditions

Figure 16 depicts the w, or normal deflection, modal shapes for the above mixed-series solutions. The effects of noncircularity are obvious for axial loading, with the shape changing considerably in appearance with increasing eccentricity, corresponding to a reduction to less than half the buckling loading. For the noncircular cases, the deflections are greatest in the left hand parts of the panels where the radius of curvature has greater value, which is reasonable. In the case of lateral pressure buckling, the modal shapes remain somewhat similar for the different values of ξ, and only those for the extreme values of ξ are shown. This is probably due to the normal pressure loading, which should tend to decrease the curvature in the flatter parts of the panel. (The relatively smaller u and v modal shapes do indicate more definitely the varying curvature of the panels.) It is possible that buckling modes other than those considered might give lower buckling loadings for the same value of the eccentricity parameter ξ. However, this was not pursued in the present study.

4.2.3 Effects of Boundary Conditions Upon Buckling Loadings

The boundary conditions along the straight edges of the panel considered in the previous sections were changed from the familiar simply supported conditions, equations (2.15-2.18), to the restricted simply supported conditions,

equations (2.19, 2.16-2.18). This represents cancelling transverse motion of the straight edges.

The buckling loadings are given in Figure 17, and the ratio of increase due to the more restricted boundary conditions is indicated in Figure 18, both plotted against the eccentricity parameter, ξ. The corresponding modal shapes are shown in Figure 19.

The case of lateral pressure loading is less complicated and will be discussed first. The buckling value decreases with increasing ξ at about the same rate as in the simply supported (SS2) case as shown in Figure 17, but for a given value of ξ, the buckling loading is double or more. This is consistent with the typical modal shapes shown in Figure 19 for lateral pressure buckling, with two transverse half waves of normal deflection appearing, in place of one as in the simply supported (SS2) case. The effect of noncircularity is more evident in these modal shapes than in the simply supported case.

The results for the case of axial compression are less conclusive. Reference to Figure 14 shows that many critical loadings in this case for various values of m, the number of longitudinal half waves, and ξ, must lie relatively close together. Therefore, without exhaustive computations, it is not too meaningful, in a practical sense, to discuss the stiffening effect of the SS4 boundary conditions for one value of m, because another value of m might possibly give a lower buckling value with the same SS4 boundary conditions

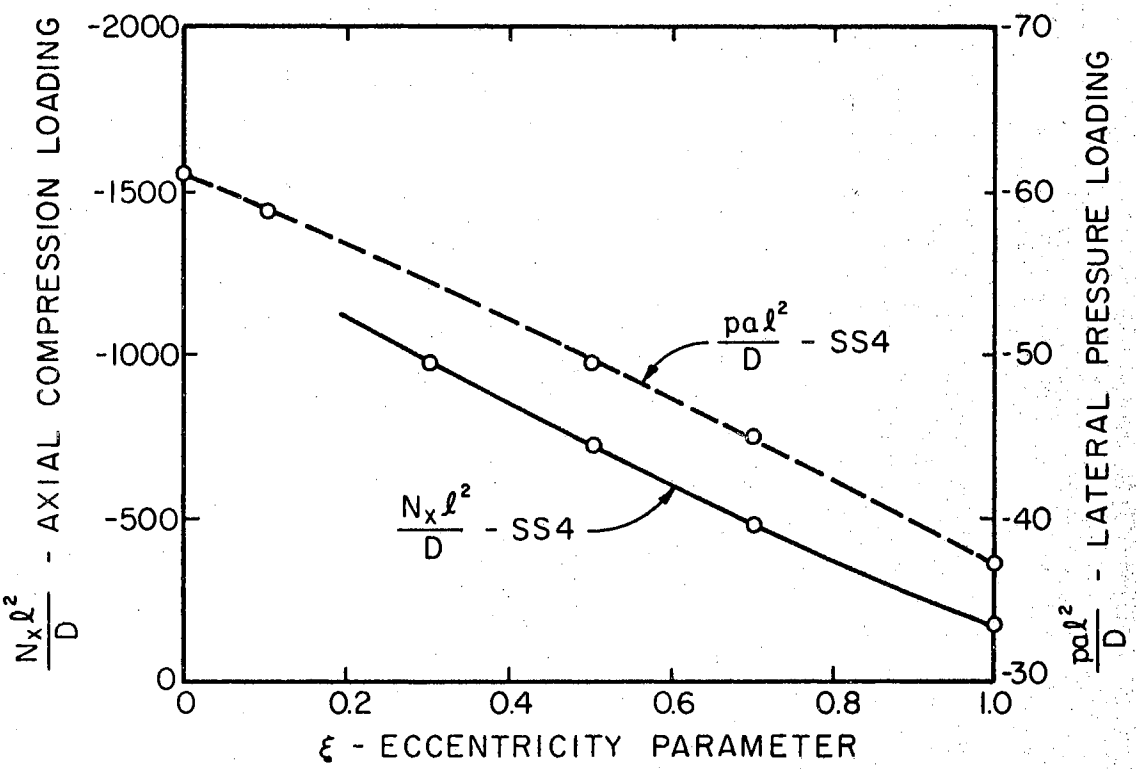

Figure 17. The Effect of Noncircularity Upon Buckling Loadings for Restricted (SS4) Boundary Conditions

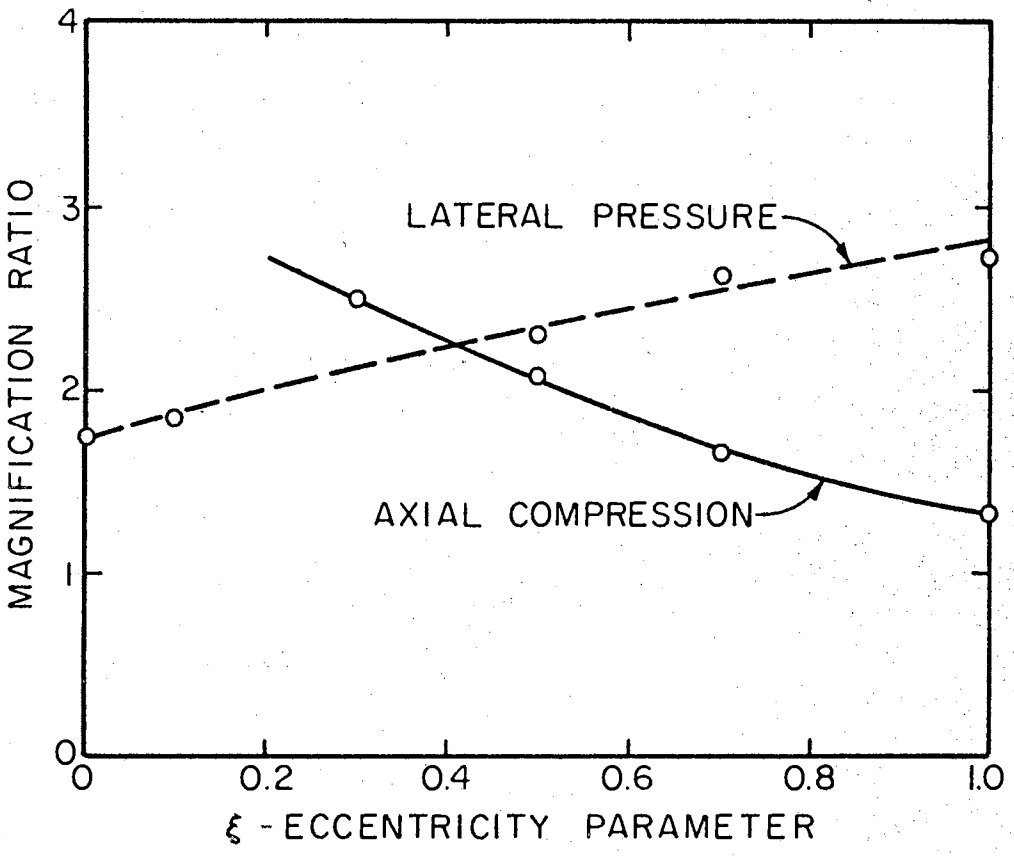

Figure 18. Magnification Ratio for Buckling Loadings Due to Cancellation of Transverse Motion Along the Straight Edges of the Panel

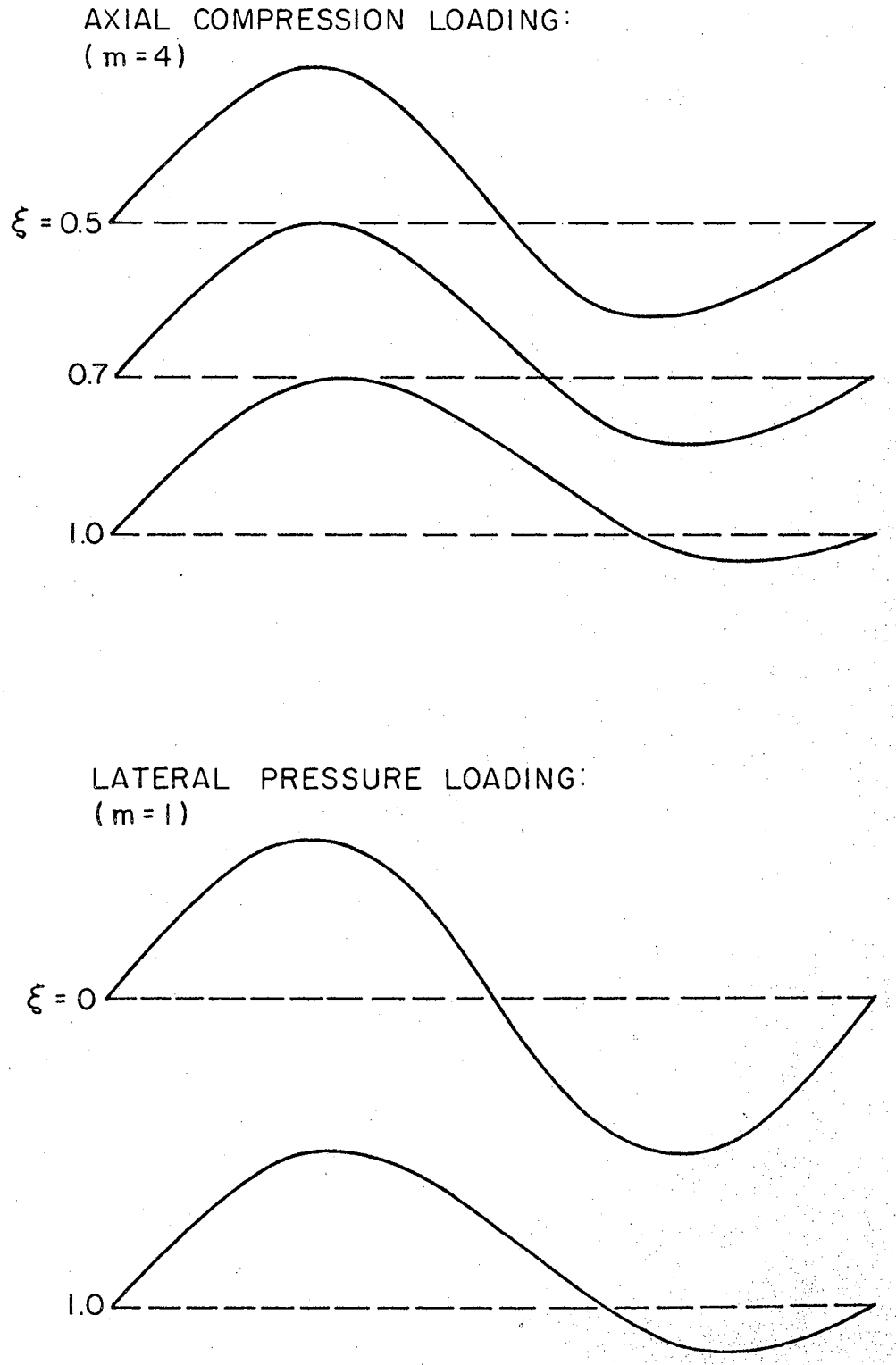

Figure 19. Normal (w) Deflection Modal Shapes for Axial Loading and for Lateral Pressure Loading, with Restricted (SS4) Boundary Conditions

and for the same value of ξ.

However, a few calculations were made for m = 4, to produce a possible buckling mode which might be the result of changing to the stiffer boundary conditions. These results are shown in Figures 17, 18, and 19. The axial loading decreases relatively more rapidly with increasing eccentricity than in the SS2 simply supported case and this is reflected in Figure 18, where the magnification ratio decreases with increasing eccentricity. The w modal shapes, Figure 19, are reminiscent of the SS2 case.

4.3 Summary of Results

The mixed-series approach to the solution of the buckling problem for cylindrical panels has been tested and demonstrated in the preceding sections. In section 4.1.2, the method is tested by comparison with the buckling problem solution, for a simply supported (SS2) axially compressed circular cylindrical panel, obtained by the substitution of double trigonometric series into the Donnell stability equations. Agreement is good (see Table I). A few trial calculations were made for the same panel with restricted simply supported (SS4) boundary conditions along the straight edges. Then the method was checked with the results of others (3) for an axially loaded panel with free straight edges and it agreed well.

In the following sections 4.1.3, 4.1.4, and 4.2.1, the method was checked for a variety of cases. In 4.1.3, the

method agreed well with results (4) obtained for a circular cylindrical panel under normal pressure loading. Singer et al. (4) calculated the SS2 answers by using the uncoupled Donnell equations and calculated the SS4 answers by using the escalated eighth order form of the Donnell equations.

In section 4.1.4, the method agreed well with results obtained by Kempner and Chen (10) for an axially loaded oval cylindrical shell. In effect, one quarter of a closed doubly symmetrical noncircular shell was treated as a panel with appropriate boundary conditions along the straight edges (see Figure 11).

Section 4.2 demonstrates the application of the mixed-series approach to a typical cylindrical panel. Comparison with the double trigonometric series solution, as presented by Timoshenko (13), checked satisfactorily the calculations for combined loading by lateral pressure and axial compression for the simply supported circular cylindrical case. Subsequent calculations indicated the trends in buckling loading and modal shape produced by noncircularity and by stiffening the boundary conditions along the straight edges.

The SS2 examples calculated had the same initial value for curvature and the curvature increased in a sinusoidal manner along the transverse direction to the maximum value. A good engineering approximation for the buckling loading is derived by regarding such noncircular panels as circular panels with the respective minimum value curvatures. The

modal shapes for the axial loading case were affected more by noncircularity than for the pressure loading case. Changing the simply supported (SS2) boundary conditions to the restricted (SS4) conditions along the straight edges produced considerably higher buckling loadings for both cases for the range of noncircularity considered. The modal shapes were also modified. Care is suggested in making predictions of the buckling mode to be expected when boundary conditions are changed since solutions for various values of m may be relatively close to one another.

Computation time on the IBM 360 varied from about six to twelve minutes each for the data points of the cases considered in the present work. Some experience in using the computer program is necessary to conserve computer time. The usual compromises between the computation time required and the accuracy come into consideration, and some additional general statements can be made. The time required increases with the number of waves present, and with the relative width of the panel. Conversely, the computation time is less for relatively longer panels.

CHAPTER V

SUMMARY AND CONCLUSIONS

The combined power series--trigonometric series approach solves the linear stability problem for circular or noncircular cylindrical panels with arbitrary boundary conditions along the straight edges and simply supported boundary conditions along the curved edges. With the wide variety of possible cases and with the computation time that is required, it appears more practical to consider individual panel buckling problems as they arise rather than to generate comprehensive results.

The method is based upon the substitution of a mixed-series into equations analogous to Donnell's stability equations. The only additional feature in the equations is the consideration of a variable radius of curvature, expressed in terms of a power series. Use of combined trigonometric-power series also allows treatment of any boundary conditions along the straight edges of the panel.

Comparison with the results of other investigators tested the method and the comparison was good. The application of the method was demonstrated by studying the effects of noncircularity and boundary conditions upon the stability behavior of a typical panel under axial

compression and under lateral pressure loading. In general terms, the buckling loading is changed by noncircularity and is approximated well by considering the panel to be a circular cylindrical panel with a radius equal to the actual maximum value. Buckling loadings are increased for non-circular panels by applying more restrictive boundary conditions.

It appears simple in theory to extend this method to cases with additional cross sectional properties, besides the radius of curvature, varying in the transverse direction. Some improvements in the method might be made to reduce the computation time. The most obvious goal would be to seek some escalated form of the third equilibrium equation (2.3) in order to uncouple the equations (2.1 - 2.3) and to reduce the number of unknowns, and hence, the computation time. However, in order to do this, it would be necessary also to account for the boundary conditions and this seems difficult. For longer panels, the Donnell equations become inaccurate (6, p. 228), but with the present method, more elaborate basic equations may easily be used.

The method corroborated the results of others for a variety of cases and it is a useful tool for the investigation of the linear buckling of cylindrical panels.

A SELECTED BIBLIOGRAPHY

(1) Langhaar, H. "General Theory of Buckling." Applied Mechanics Reviews, Vol. 11, No. 11, Nov. 1958, pp. 585-588.

(2) Batdorf, S. "A Simplified Method of Elastic Stability Analysis for Thin Cylindrical Shells." NACA Report No. 874, 1947.

(3) Chu, K., and G. Krishnamoorthy. "Buckling of Open Cylindrical Shells." Journal of the Engineering Mechanics Division, ASCE, April 1967, pp. 177-203.

(4) Singer, J., A. Meer, and M. Baruch. "Buckling of Cylindrical Panels Under Lateral Pressure." Technion Research and Development Foundation, TAE Report No. 85, Haifa, Israel, 1968.

(5) Donnell, L. "Stability of Thin-Walled Tubes Under Torsion." NACA Report No. 479, 1933.

(6) Kraus, H. Thin Elastic Shells. New York: John Wiley and Sons, Inc., 1967.

(7) Marguerre, K. "Stabilitat der Zylinderschale veranderlicher Krummung." NACA Tech. Memo. No. 1302, 1951.

(8) Kempner, J., and F. Romano. "Stresses in Short Noncircular Cylindrical Shells Under Lateral Pressure." Journal of Applied Mechanics, Trans. ASME, Vol. 29, No. 4, Dec. 1962, pp. 669-674.

(9) Kempner, J. "Unified Thin-Shell Theory." Polytechnic Inst. of Brooklyn, PIBAL Report No. 566, 1960.

(10) Kempner, J., and Y. Chen. "Buckling and Postbuckling of an Axially Compressed Oval Cylindrical Shell." Polytechnic Inst. of Brooklyn, PIBAL Report No. 917, 1966.

(11) Boyd, D. "Analysis of Open Noncircular Cylindrical Shells." AIAA Journal, Vol. 7, No. 3, 1969.

(12) Batdorf, S. "On the Application of Inverse Differential Operators to the Solution of Cylinder Buckling and Other Problems." AIAA/ASME 10th Structures, Structural Dynamics, and Materials Conferences, New Orleans, April 14-16, 1969.

(13) Timoshenko, S., and J. Gere. Theory of Elastic Stability. New York: McGraw-Hill Book Company, Inc., 1961.

(14) Rehfield, L., and W. Hallauer. "Edge Restraint Effect on Buckling of Compressed Curved Panels." AIAA Journal, Vol. 6, No. 1, Jan. 1968, pp. 187-189.

(15) Novozhilov, V. Foundations of the Nonlinear Theory of Elasticity. Rochester: Graylock Press, 1953, pp. 52-53.

APPENDIX A

DERIVATION OF BASIC EQUATIONS

We derive in this Appendix A the basic equations used in this classical-buckling study of cylindrical shells. We consider thin shells of constant thickness made of homogeneous isotropic elastic material. To give an overall perspective, the equations are derived from an energy standpoint and the equilibrium equations and the stability equations are presented for the above-mentioned class of shells, along with appropriate boundary conditions. Surface loadings, edge loadings and thermal loadings are included.

The bases for the equations are the Kirchhoff-Love hypothesis of nondeformable normals and the assumption of plane stress in the thin shell wall. Further restrictions to be applied are the small-deflection assumption, and Donnell-type assumptions in rotation-displacement relations.

Therefore, for a thin shell with negligible transverse shear deformation, the displacements at a point in the shell wall (s,x,z) are

$$\begin{aligned} v &= v_z = v_o + z\omega_x \\ u &= u_z = u_o - z\omega_s \\ w &= w_z = w_o \end{aligned} \qquad \text{(A.1)}$$

(Please refer to Figure 1.) The displacement components are

v, u, and w in the positive s, x, and z directions, respectively, and the rotation components are the rotations of a nondeformable normal about tangents to the respective lines of constant s or x. The subscript o refers to the middle surface value. The strain-displacement relations for small deformations and rotations are, where e represents classical small-displacement strain:

$$\begin{aligned} e_s &= e_{s_o} + zk_s \\ e_x &= e_{x_o} + zk_x \\ e_{sx} &= e_{sx_o} + 2zk_{sx} \end{aligned} \tag{A.2}$$

where

$$\begin{aligned} e_{s_o} &= \frac{\partial v_o}{\partial s} + \frac{w}{r} \quad , \quad k_s = \frac{\partial \omega_x}{\partial s} \\ e_{x_o} &= \frac{\partial u_o}{\partial x} \quad , \quad k_x = -\frac{\partial \omega_s}{\partial x} \\ e_{sx_o} &= \frac{\partial v_o}{\partial x} + \frac{\partial u_o}{\partial s} \quad , \quad k_{sx} = \tfrac{1}{2}\left[\frac{\partial \omega_x}{\partial x} - \frac{\partial \omega_s}{\partial s}\right] . \end{aligned} \tag{A.3}$$

The rotation components are

$$\omega_s = \frac{\partial w}{\partial x} \quad , \quad \omega_x = \frac{v_o}{r} - \frac{\partial w}{\partial s} \tag{A.4}$$

or for cases in which the Donnell-type assumptions are applicable:

$$\omega_s = \frac{\partial w}{\partial x} \quad , \quad \omega_x = -\frac{\partial w}{\partial s} \ . \tag{A.5}$$

For cases involving buckling and postbuckling, the following strain-displacement relations are called for (see Ref. 15):

$$\begin{aligned} \varepsilon_s &= e_s + \tfrac{1}{2}\omega_x^2 \\ \varepsilon_x &= e_x + \tfrac{1}{2}\omega_s^2 \\ \gamma_{sx} &= e_{sx} - \omega_s\omega_x \quad . \end{aligned} \tag{A.6}$$

These are considered sufficiently accurate for analysis of thin shells where deformations and rotations are small and deformations are small compared to rotations (see Ref. 9):

$$\varepsilon = O(e) = O(\omega^2) \ll 1 \quad .$$

The general stress-strain relations are assumed as given below, in a familiar form. The symbols σ and τ represent normal and shear stress, respectively, and E is Young's modulus, T is temperature, ν is Poisson's ratio and α is the thermal expansion coefficient:

$$\begin{aligned} \sigma_s &= \frac{E}{1-\nu^2}\left[\varepsilon_s + \nu\varepsilon_x - (1+\nu)\alpha T\right] \\ \sigma_x &= \frac{E}{1-\nu^2}\left[\varepsilon_x + \nu\varepsilon_s - (1+\nu)\alpha T\right] \\ \tau_{xs} &= \frac{E}{2(1+\nu)}\,\gamma_{xs} \quad . \end{aligned} \tag{A.7}$$

The force and moment resultants are, with the thin-shell assumption that $z \ll R$:

$$N_s = \int_{-\frac{h}{2}}^{\frac{h}{2}} \sigma_s \, dz$$

$$N_x = \int_{-\frac{h}{2}}^{\frac{h}{2}} \sigma_x \, dz$$

$$M_s = \int_{-\frac{h}{2}}^{\frac{h}{2}} \sigma_s z dz$$

$$M_x = \int_{-\frac{h}{2}}^{\frac{h}{2}} \sigma_x z dz$$

$$N_{xs} = N_{sx} = \int_{-\frac{h}{2}}^{\frac{h}{2}} \tau_{sx}\, dz$$

$$M_{sx} = M_{xs} = \int_{-\frac{h}{2}}^{\frac{h}{2}} \tau_{xs} z dz \quad , \qquad \text{(A.8)}$$

where h is the shell thickness. Recasting the above equations into the form of force- and moment-resultant-strain relations results in:

$$N_s = \frac{Eh}{1-\nu^2} [\epsilon_s + \nu\epsilon_x - (1+\nu)\alpha T]$$

$$N_x = \frac{Eh}{1-\nu^2} [\epsilon_x + \nu\epsilon_s - (1+\nu)\alpha T]$$

$$N_{sx} = N_{xs} = Gh\,\gamma_{sx}$$

$$M_s = D(k_s + \nu k_x) - M_T \qquad \text{(A.9)}$$

$$M_x = D(k_x + \nu k_s) - M_T$$

$$M_{sx} = M_{xs} = (1-\nu) D\, k_{sx}$$

where D is the flexural rigidity $\frac{Eh^3}{12(1-\nu^2)}$, G is the shearing modulus $E/2(1+\nu)$, and

$$M_T = (1+\nu)\alpha \int_{-\frac{h}{2}}^{\frac{h}{2}} Tz\,dz \quad . \tag{A.10}$$

With all the above presented, one may now consider energy methods in order to derive the equilibrium and stability equations. By definition, the internal strain energy, U, stored in a body under conditions of plane stress is

$$U = \tfrac{1}{2}\iiint [\sigma_s \varepsilon_s + \sigma_x \varepsilon_x + \tau_{sx} \gamma_{sx} - \frac{E(1+\nu)}{(1-\nu^2)} \alpha T(\varepsilon_s+\varepsilon_x)]\,ds\,dx\,dz \quad . \tag{A.11}$$

Consider the shell to be in a state of equilibrium, denoted by superscript o, with the equilibrium displacements v^o, u^o, w^o. Suppose that the shell can be further displaced by an admissible set of displacements denoted by superscript ': v', u', w'. Allow such a displacement that the total displacement can be written as follows:

$$v^o + \lambda v' \quad , \quad u^o + \lambda u' \quad , \quad w^o + \lambda w' \quad ,$$

where λ is a small arbitrary scalar factor. After substitution of this displacement distribution into the strain energy expression, and neglect of terms of higher order than λ^2, we may write the result as

$$U = U^o + \lambda U' + \lambda^2 U'' \tag{A.12}$$

where

$$U^o = \tfrac{1}{2}\iiint [\sigma_s{}^o \varepsilon_s{}^o + \sigma_x{}^o \varepsilon_x{}^o + \tau_{sx}{}^o \gamma_{sx}{}^o - \frac{E\alpha T}{(1-\nu)} (\varepsilon_s{}^o + \varepsilon_x{}^o)]\,ds\,dx\,dz$$

$$U' = \iiint [\sigma_s^{\,o} \varepsilon_s' + \sigma_x^{\,o} \varepsilon_x' + \tau_{sx}^{\,o} \gamma_{sx}'] ds\,dx\,dz$$

$$U'' = \tfrac{1}{2} \iiint [\sigma_s' \varepsilon_s' + \sigma_x' \varepsilon_x' + \tau_{sx}' \gamma_{sx}' + 2(\sigma_s^{\,o} \varepsilon_s'' + \sigma_x^{\,o} \varepsilon_x'' + \tau_{sx}^{\,o} \gamma_{sx}'')] ds\,dx\,dz \quad . \tag{A.13}$$

We have made use of the following definitions, with e and ω defined as before:

$$\varepsilon_s^{\,o} = e_s^{\,o} + \tfrac{1}{2}\omega_x^{\,o\,2}, \quad \varepsilon_x^{\,o} = e_x^{\,o} + \tfrac{1}{2}\omega_s^{\,o\,2},$$

$$\gamma_{sx}^{\,o} = e_{sx}^{\,o} - \omega_s^{\,o}\omega_x^{\,o}$$

$$\varepsilon_s' = e_s' + \omega_x^{\,o}\omega_x', \quad \varepsilon_x' = e_x' + \omega_s^{\,o}\omega_s',$$

$$\gamma_{sx}' = e_{sx}' - \omega_s^{\,o}\omega_x' - \omega_s'\omega_x^{\,o}$$

$$\varepsilon_s'' = \tfrac{1}{2}\omega_s'^{\,2}, \quad \varepsilon_x'' = \tfrac{1}{2}\omega_x'^{\,2}, \quad \gamma_{sx}'' = -\omega_s'\omega_x'$$

$$\sigma_s^{\,o} = \frac{E}{1-\nu^2}[\varepsilon_s^{\,o} + \nu\varepsilon_x^{\,o} - (1+\nu)\alpha T]$$

$$\sigma_x^{\,o} = \frac{E}{1-\nu^2}[\varepsilon_x^{\,o} + \nu\varepsilon_s^{\,o} - (1+\nu)\alpha T] \tag{A.14}$$

$$\tau_{sx}^{\,o} = G\gamma_{sx}^{\,o}$$

$$\sigma_s' = \frac{E}{1-\nu^2}(\varepsilon_s' + \nu\varepsilon_x'), \quad \sigma_x' = \frac{E}{1-\nu^2}(\varepsilon_x' + \nu\varepsilon_s')$$

$$\tau_{sx}' = G\gamma_{sx}'$$

$$\sigma_s'' = \frac{E}{1-\nu^2}(\varepsilon_s'' + \nu\varepsilon_x''), \quad \sigma_x'' = \frac{E}{1-\nu^2}(\varepsilon_x'' + \nu\varepsilon_s'')$$

$$\tau_{sx}'' = G\gamma_{sx}'' \quad .$$

Also the total stresses and strains in the adjacent state of equilibrium may be written:

$$
\begin{aligned}
\sigma_s &= \sigma_s^{\,o} + \lambda\sigma_s' + \lambda^2\sigma_s'' \\
\sigma_x &= \sigma_x^{\,o} + \lambda\sigma_x' + \lambda^2\sigma_x'' \\
\tau_{sx} &= \tau_{sx}^{\,o} + \lambda\tau_{sx}' + \lambda^2\tau_{sx}'' \\
\epsilon_s &= \epsilon_s^{\,o} + \lambda\epsilon_s' + \lambda^2\epsilon_s'' \\
\epsilon_x &= \epsilon_x^{\,o} + \lambda\epsilon_x' + \lambda^2\epsilon_x'' \\
\gamma_{sx} &= \gamma_{sx}^{\,o} + \lambda\gamma_{sx}' + \lambda^2\gamma_{sx}'' \quad .
\end{aligned}
\tag{A.15}
$$

For a state of stable equilibrium in the adjacent equilibrium state:

$$\Delta U + \Delta V > 0 \tag{A.16}$$

where ΔV equals the negative work done by edge and surface forces (which forces may be functions of the displacements). This may be rewritten as follows:

$$\Delta U + \Delta V = \lambda(\delta U' + \delta V') + \lambda^2(\delta U'' + \delta V'') + O(\lambda^3).$$

If λ is arbitrary, $\delta U' + \delta V'$ must be equal to zero in order for $\Delta U + \Delta V$ to be positive. Then since λ^2 is positive, $\delta U'' + \delta V''$ must be greater than zero for stable equilibrium. Then the critical configuration for neutral stability must be the set of displacements and rotations for which $\delta U'' + \delta V'' = 0$. It happens that the first relation $\delta U' + \delta V' = 0$ gives the equilibrium equations for the basic state and the second relation $\delta U'' + \delta V'' = 0$ gives the stability equations for the buckled-state displacements and rotations. We will apply these principles to a rather general case of noncircular cylindrical shells and then specialize the results to arrive at the simplified equations studied in this work.

In order to derive the equilibrium equations, we consider the first relation $\delta U' + \delta V' = 0$. Calculating the first variation of strain energy U' gives:

$$\delta U' = -\iint\Bigg[\left(\frac{\partial N_x^{\,o}}{\partial x} + \frac{\partial N_{sx}^{\,o}}{\partial s}\right)\delta u' + \left(\frac{\partial N_s^{\,o}}{\partial s} + \frac{\partial N_{sx}^{\,o}}{\partial x}\right)\delta v' - \frac{N_s^{\,o}}{r}\,\delta w' +$$
$$+ \left(-\frac{\partial M_x^{\,o}}{\partial x} - \frac{\partial M_{sx}^{\,o}}{\partial s} - N_x^{\,o}\omega_s^{\,o} + N_{sx}^{\,o}\omega_x^{\,o}\right)\delta\omega_s' +$$
$$+ \left(\frac{\partial M_s^{\,o}}{\partial s} + \frac{\partial M_{xs}^{\,o}}{\partial x} - N_s^{\,o}\omega_x^{\,o} + N_{sx}^{\,o}\omega_s^{\,o}\right)\delta\omega_x'\Bigg]\,dsdx + \tag{A.17}$$
$$+ \int (N_{sx}^{\,o}\delta v' + N_x^{\,o}\delta u' - M_x^{\,o}\delta\omega_s' + M_{xs}^{\,o}\delta\omega_x')\Big|_{x_1}^{x_2} ds +$$
$$+ \int (N_s^{\,o}\delta v' + N_{sx}^{\,o}\delta u' + M_s^{\,o}\delta\omega_x' - M_{sx}^{\,o}\delta\omega_s')\Big|_{s_1}^{s_2} dx .$$

The first variation of the work done by the internal shear forces may be written:

$$\delta W_Q = \iint\left[\frac{Q_s^{\,o}}{r}\,\delta v' + \left(\frac{\partial Q_s^{\,o}}{\partial s} + \frac{\partial Q_x^{\,o}}{\partial x}\right)\delta w' + Q_x^{\,o}\delta\omega_s' - Q_s^{\,o}\delta\omega_x'\right]dsdx$$
$$- \int Q_x^{\,o}\delta w'\Big|_{x_1}^{x_2} ds - \int Q_s^{\,o}\delta w'\Big|_{s_1}^{s_2} dx . \tag{A.18}$$

The first variation of the work done by the external surface forces is

$$\delta W_S = \iint(F_s\delta v' + F_x\delta u' + F_z\delta w')\,dsdx \tag{A.19}$$

where the F-components may be functions of position on the middle surface and in the case of large deflections, also functions of the displacements. For the work done by the edge forces, denoted by the bars, we have:

$$\delta W_E =$$

on edges of constant s,

$$\int(\bar{N}_s\delta v' + \bar{N}_{sx}\delta u' + \bar{Q}_s\delta w' + \bar{M}_s\delta\omega_x' - \bar{M}_{sx}\delta\omega_s')dx + \qquad (A.20)$$

on edges of constant x,

$$+ \int(\bar{N}_{xs}\delta v' + \bar{N}_x\delta u' + \bar{Q}_x\delta w' - \bar{M}_x\delta\omega_s' + \bar{M}_{xs}\delta\omega_x')ds \ .$$

After consideration of the relation $\delta U' - \delta W' = 0$ and the arbitrariness of $\delta u'$, $\delta v'$, $\delta w'$, etc., we can set forth the following Euler's equations and boundary conditions:

$$\frac{\partial N_x^{\,o}}{\partial x} + \frac{\partial N_{sx}^{\,o}}{\partial s} + F_x = 0$$

$$\frac{\partial N_s^{\,o}}{\partial s} + \frac{\partial N_{xs}^{\,o}}{\partial x} + \frac{1}{r}\left[\frac{\partial M_s^{\,o}}{\partial s} + \frac{\partial M_{xs}^{\,o}}{\partial x} - N_s^{\,o}\omega_x^{\,o} + N_{sx}^{\,o}\omega_s^{\,o}\right] + F_s = 0 \qquad (A.21)$$

$$\frac{\partial}{\partial x}\left[\frac{\partial M_x^{\,o}}{\partial x} + \frac{\partial M_{sx}^{\,o}}{\partial s} + N_x^{\,o}\omega_s^{\,o} - N_{sx}^{\,o}\omega_x^{\,o}\right] + \frac{\partial}{\partial s}\left[\frac{\partial M_s^{\,o}}{\partial s} + \frac{\partial M_{sx}^{\,o}}{\partial x} - N_s^{\,o}\omega_x^{\,o} + N_{sx}^{\,o}\omega_s^{\,o}\right] - \frac{N_s^{\,o}}{r} + F_z = 0 \ .$$

The above comprise the large-deflection equilibrium equations and the boundary conditions associated with these are as follows:

on sides of constant s,

$$N_s^{\,o} - \bar{N}_s + \frac{1}{r}(M_s^{\,o} - \bar{M}_s) = 0 \quad \text{or} \quad \delta v' = 0$$

$$N_{sx}^{\,o} - \bar{N}_{sx} = 0 \quad \text{or} \quad \delta u' = 0$$

$$Q_s^{\,o} - \bar{Q}_s + \frac{\partial}{\partial x}(M_{sx}^{\,o} - \bar{M}_{sx}) = 0 \quad \text{or} \quad \delta w' = 0$$

$$M_s^{\,o} = \bar{M}_s = 0 \quad \text{or} \quad \delta\left(\frac{\partial w'}{\partial s}\right) = 0$$

at corners

$$x = x_1 \ , \quad x = x_2,$$

$$M_{sx}^{\,o} - \bar{M}_{sx} = 0 \quad \text{or} \quad \delta w' = 0 \tag{A.22}$$

on sides of constant x,

$$N_{xs}^{\,o} - \bar{N}_{xs} + \frac{1}{r}(M_{xs}^{\,o} - \bar{M}_{xs}) = 0 \quad \text{or} \quad \delta v' = 0$$

$$N_x^{\,o} - \bar{N}_x = 0 \quad \text{or} \quad \delta u' = 0$$

$$Q_x^{\,o} - \bar{Q}_x + \frac{\partial}{\partial s}(M_{xs}^{\,o} - \bar{M}_{xs}) = 0 \quad \text{or} \quad \delta w' = 0$$

$$M_x^{\,o} - \bar{M}_x = 0 \quad \text{or} \quad \delta\left(\frac{\partial w'}{\partial x}\right) = 0$$

at corners

$$s = s_1, \ s = s_2,$$

$$M_{xs}^{\,o} - \bar{M}_{xs} = 0 \quad \text{or} \quad \delta w' = 0 \ .$$

Linearization of the above large-deflection equilibrium equations, by dropping those terms containing w^o explicitly and by dropping terms containing w^o in the stress resultant expressions, results in the classical equilibrium equations:

$$\begin{aligned}
&\frac{\partial N_x^{\,o}}{\partial x} + \frac{\partial N_{sx}^{\,o}}{\partial s} + F_x = 0 \\
&\frac{\partial N_s^{\,o}}{\partial s} + \frac{\partial N_{xs}^{\,o}}{\partial x} + \frac{1}{r}\left(\frac{\partial M_s^{\,o}}{\partial s} + \frac{\partial M_{sx}^{\,o}}{\partial x}\right) + F_s = 0 \\
&\frac{\partial}{\partial s}\left(\frac{\partial M_x^{\,o}}{\partial x} + \frac{\partial M_{sx}^{\,o}}{\partial s}\right) + \frac{\partial}{\partial s}\left(\frac{\partial M_s^{\,o}}{\partial s} + \frac{\partial M_{xs}^{\,o}}{\partial x}\right) - \frac{N_s^{\,o}}{r} + F_z = 0 \ .
\end{aligned} \tag{A.23}$$

An additional simplification is the adoption of the Donnell-type assumptions, equations (A.5). Changes are reflected in the internal work done by shear forces:

$$\delta W_Q = \iint \left[\left(\frac{\partial Q_s^{\,o}}{\partial s} + \frac{\partial Q_x^{\,o}}{\partial x} \right) \delta w' + Q_x^{\,o} \delta \omega_s' - Q_s^{\,o} \delta \omega_x' \right] dx ds -$$

$$- \int_s Q_x^{\,o} \delta w' \Big|_{x_1}^{x_2} ds - \int Q_s^{\,o} \delta w' \Big|_{s_1}^{s_2} dx \quad . \qquad \text{(A.24)}$$

This simplification is then reflected in the absence of the transverse shear term in the second of equations (A.23). The corresponding boundary conditions for this case are:

on sides of constant s,

$$N_s^{\,o} - \bar{N}_s = 0 \qquad \text{or} \quad \delta v' = 0$$

$$N_{sx}^{\,o} - \bar{N}_{sx} = 0 \qquad \text{or} \quad \delta u' = 0$$

$$Q_s^{\,o} - \bar{Q}_s + \frac{\partial}{\partial x}(M_{sx}^{\,o} - \bar{M}_{sx}) = 0 \quad \text{or} \quad \delta w' = 0$$

$$M_s^{\,o} - \bar{M}_s = 0 \qquad \text{or} \quad \delta \left(\frac{\partial w'}{\partial s} \right) = 0$$

at corners

$$x = x_1 \ , \quad x = x_2 ,$$

$$M_{sx}^{\,o} - \bar{M}_{sx} = 0 \quad \text{or} \quad \delta w' = 0 \qquad \text{(A.25)}$$

on sides of constant x,

$$N_{xs}^{\,o} - \bar{N}_{xs} = 0 \qquad \text{or} \quad \delta v' = 0$$

$$N_x^{\,o} - \bar{N}_x = 0 \qquad \text{or} \quad \delta u' = 0$$

$$Q_x^{\,o} - \bar{Q}_x + \frac{\partial}{\partial s}(M_{xs}^{\,o} - \bar{M}_{xs}) \qquad \text{or} \quad \delta w' = 0$$

$$M_x^{\,o} - \bar{M}_x = 0 \qquad \text{or} \quad \delta \left(\frac{\partial w'}{\partial x} \right) = 0$$

at corners

$$s = s_1 \quad , \quad s = s_2 \quad ,$$

$$M_{xs}^{\,o} - \bar{M}_{xs} = 0 \quad \text{or} \quad \delta w' = 0 \quad .$$

The Donnell-type assumptions can also be applied to the large-deflection equilibrium equations themselves. This results in the following set of equations:

$$\begin{aligned}
&\frac{\partial N_x^{\,o}}{\partial x} + \frac{\partial N_{sx}^{\,o}}{\partial s} + F_x = 0 \\
&\frac{\partial N_s^{\,o}}{\partial s} + \frac{\partial N_{xs}^{\,o}}{\partial x} + F_s = 0 \\
&\frac{\partial}{\partial s}\left(\frac{\partial M_s^{\,o}}{\partial s} + \frac{\partial M_{xs}^{\,o}}{\partial x} - N_s^{\,o}\omega_x^{\,o} + N_{sx}^{\,o}\omega_s^{\,o}\right) + \\
&+ \frac{\partial}{\partial x}\left(\frac{\partial M_x^{\,o}}{\partial x} + \frac{\partial M_{sx}^{\,o}}{\partial s} + N_x^{\,o}\omega_s^{\,o} - N_{sx}^{\,o}\omega_x^{\,o}\right) - \frac{N_s^{\,o}}{r} + F_z = 0
\end{aligned} \tag{A.26}$$

where the first two equations are identical in form to the corresponding classical equilibrium equations and the third equation is similar in form to the third of equations (A.21). The Donnell-type assumptions will also enter into the moment stress-resultant expressions, and change the boundary conditions as well.

The above equations give the equilibrium displacements and stresses due to the applied loads. Whether or not such a state of equilibrium is stable or unstable is decided by equation (A.16). The critical state occurs when

$$\delta U'' + \delta V'' = 0$$

and this criterion may be used to determine the critical values of the loadings and the associated displacements,

v', u', and w'. Proceeding as before, performing the first variation of the strain energy and the work integral V", and with the surface loadings, F, dependent on possibly both the sets of displacements, we obtain:

$$\frac{\partial N_x'}{\partial x} + \frac{\partial N_{sx}'}{\partial s} + F_x = 0$$

$$\frac{\partial N_s'}{\partial s} + \frac{\partial N_{xs}'}{\partial x} + \frac{1}{r}\left(\frac{\partial M_s'}{\partial s} + \frac{\partial M_{xs}'}{\partial x} - N_s^{\circ}\omega_x' - N_s'\omega_x^{\circ} + N_{sx}^{\circ}\omega_s' + N_{sx}'\omega_s^{\circ}\right) + F_s = 0$$

$$\frac{\partial}{\partial s}\left(\frac{\partial M_s'}{\partial s} + \frac{\partial M_{xs}'}{\partial x} - N_s^{\circ}\omega_x' - N_s'\omega_x^{\circ} + N_{sx}^{\circ}\omega_s' + N_{sx}'\omega_s^{\circ}\right) + \frac{\partial}{\partial x}\left(\frac{\partial M_x'}{\partial x} + \frac{\partial M_{sx}'}{\partial s} + N_x^{\circ}\omega_s' + N_x'\omega_s^{\circ} - N_{xs}^{\circ}\omega_x' - N_{xs}'\omega_x^{\circ}\right) - \frac{N_s'}{r} + F_z = 0 \quad . \qquad (A.27)$$

The associated boundary conditions are given by:

on sides of constant s,

$$N_s' + \frac{M_s'}{r} = 0 \qquad \text{or} \quad \delta v' = 0$$

$$N_{sx}' = 0 \qquad \text{or} \quad \delta u' = 0$$

$$\left(\frac{\partial M_s'}{\partial s} + 2\frac{\partial M_{sx}'}{\partial x} - N_s^{\circ}\omega_x' - N_s'\omega_x^{\circ} + N_{sx}^{\circ}\omega_s' + N_{sx}'\omega_s^{\circ}\right) = 0$$

$$\text{or} \quad \delta w' = 0$$

$$M_s' = 0 \qquad \text{or} \quad \delta\left(\frac{\partial w'}{\partial s}\right) = 0$$

at corners

$$x = x_1 \quad , \quad x = x_2 \quad ,$$

$$M_{sx}'\big|_{x = x_2} = M_{sx}'\big|_{x = x_1} \qquad \text{or} \quad \delta w' = 0$$

on sides of constant x,

$$N_{xs}' + \frac{M_{xs}'}{r} = 0 \qquad \text{or} \quad \delta v' = 0$$

$$N_x' = 0 \qquad \text{or} \quad \delta u' = 0$$

$$\frac{\partial M_x'}{\partial x} + 2\frac{\partial M_{sx}'}{\partial s} + N_x^{\,o}\omega_s' + N_x'\omega_s^{\,o} - N_{xs}^{\,o}\omega_x' - N_{xs}'\omega_x^{\,o} = 0 \qquad \text{(A.28)}$$

$$\text{or} \quad \delta w' = 0$$

$$M_x' = 0 \qquad \text{or} \quad \delta\left(\frac{\partial w'}{\partial s}\right) = 0$$

at corners

$$s = s_1 \ , \quad s = s_2 \ ,$$

$$M_{xs}'\big|_{s = s_2} = M_{xs}'\big|_{s = s_1} \qquad \text{or} \quad \delta w' = 0 \ .$$

The stability equations (A.27) are seen to be similar in form to the equilibrium equations (A.21). Knowing the equilibrium values of force and moment resultants, and if the surface loadings are at most linear functions of displacements v', u', and w', we can solve these equations for the critical values of load and temperature. These equations may be reduced using the linearizing restrictions of small displacements and the Donnell-type assumption. We remove terms explicit in ω^o in the stability equations and also terms involving ω^o in the expressions for N' and M'; this results in the following set of equations:

$$\frac{\partial N_x'}{\partial x} + \frac{\partial N_{sx}'}{\partial s} + F_x = 0$$

$$\frac{\partial N_s'}{\partial s} + \frac{\partial N_{xs}'}{\partial x} + \frac{1}{r}\left(\frac{\partial M_s'}{\partial s} + \frac{\partial M_{xs}'}{\partial x} - N_s{}^{o}\omega_x' + N_{sx}'\omega_s'\right) + F_z = 0$$

$$\frac{\partial}{\partial x}\left(\frac{\partial M_x'}{\partial x} + \frac{\partial M_{sx}'}{\partial s} + N_x{}^{o}\omega_s' - N_{xs}{}^{o}\omega_x'\right) + \qquad \text{(A.29)}$$

$$+ \frac{\partial}{\partial s}\left(\frac{\partial M_s'}{\partial s} + \frac{\partial M_{xs}'}{\partial x} - N_s{}^{o}\omega_x' + N_{sx}{}^{o}\omega_s'\right) - \frac{N_s'}{r} + F_z = 0 \ .$$

The boundary conditions associated with these equations may be gotten from equation (A.28) by a similar process. To simplify these buckling relations further one may use the Donnell-type assumption and this results in the following:

$$\frac{\partial N_x'}{\partial x} + \frac{\partial N_{sx}'}{\partial s} + F_x = 0$$

$$\frac{\partial N_s'}{\partial s} + \frac{\partial N_{xs}'}{\partial x} + F_s = 0 \qquad \text{(A.30)}$$

$$\frac{\partial}{\partial x}\left(\frac{\partial M_x'}{\partial x} + \frac{\partial M_{xs}'}{\partial s} + N_x{}^{o}\omega_s' - N_{xs}{}^{o}\omega_x'\right) +$$

$$+ \frac{\partial}{\partial s}\left(\frac{\partial M_s'}{\partial s} + \frac{\partial M_{sx}'}{\partial x} - N_s{}^{o}\omega_x' + N_{sx}{}^{o}\omega_s'\right) - \frac{N_s'}{r} + F_z = 0$$

and the associated boundary conditions become:

on sides of constant s,

$$N_s' + \frac{M_s'}{r} = 0 \qquad \text{or} \quad \delta v' = 0 \qquad \text{a.}$$

$$N_{sx}' = 0 \qquad \text{or} \quad \delta u' = 0 \qquad \text{b.}$$

$$\frac{\partial M_s'}{\partial s} + 2\frac{\partial M_{xs}'}{\partial x} - N_s{}^{c}\omega_x' + N_{sx}{}^{c}\omega_s' = 0 \quad \text{or} \quad \delta w' = 0 \qquad \text{c.}$$

$$M_s' = 0 \qquad \text{or} \quad \delta\left(\frac{\partial w'}{\partial s}\right) = 0 \qquad \text{d.}$$

at corners

$$x = x_1 \quad , \qquad x = x_2 \quad ,$$

$$M_{sx}'|_{x=x_1} = M_{sx}'|_{x_2} \quad \text{or} \quad \delta w' = 0 \qquad \text{e.}$$

(A.31)

on sides of constant x,

$$N_{sx}' + \frac{M_{sx}'}{r} = 0 \quad \text{or} \quad \delta v' = 0 \qquad \text{f.}$$

$$N_x' = 0 \quad \text{or} \quad \delta u' = 0 \qquad \text{g.}$$

$$\frac{\partial M_x'}{\partial x} + 2\frac{\partial M_{sx}'}{\partial s} + N_x{}^{o}\omega_s' - N_{xs}{}^{o}\omega_x' = 0 \quad \text{or} \quad \delta w' = 0 \qquad \text{h.}$$

$$M_x' = 0 \quad \text{or} \quad \delta\left(\frac{\partial w'}{\partial x}\right) = 0 \qquad \text{i.}$$

at corners

$$s = s_1 \quad , \qquad s = s_2 \quad ,$$

$$M_{sx}'|_{s=s_2} = M_{sx}'|_{s=s_1} \quad \text{or} \quad \delta w' = 0 \ . \qquad \text{j.}$$

The above equations for the case of a circular cylinder are the Donnell buckling equations. These equations are considered to be accurate when the buckling mode is not of an inextensible nature (Ref. 9). In the present work, we use these equations to study the buckling under axial loading and under pressure loading of cylindrical panels with curvatures readily expressible in the form of a power series. Surface loadings which are functions of displacements will not be considered and the effect of pressure loading will be taken account of by the term

$$-\frac{\partial}{\partial s}\left(N_s{}^{o}\omega_x'\right)$$

in the third equilibrium equation. The superscript prime will be dropped with the understanding that the displacements

v', u', and w' are measured from the prebuckled configuration and the N^o forces are those resultants of the prebuckled state. Temperature effects in this case are reflected in the prebuckled force values.

We may rewrite equations (A.30) using stress resultant-displacement relations:

$$\frac{\partial^2 u}{\partial x^2} + \frac{1+\nu}{2} \cdot \frac{\partial^2 v}{\partial x \partial s} + \frac{1-\nu}{2} \cdot \frac{\partial^2 u}{\partial s^2} + \frac{\nu}{r} \cdot \frac{\partial w}{\partial x} = 0$$

$$\frac{\partial^2 v}{\partial s^2} + \frac{1+\nu}{2} \cdot \frac{\partial^2 u}{\partial x \partial s} + \frac{1-\nu}{2} \cdot \frac{\partial^2 v}{\partial x^2} + \frac{\partial}{\partial s}\left(\frac{w}{r}\right) = 0 \qquad \text{(A.32)}$$

$$\nabla^4 w + \frac{12}{rh^2}\left(\frac{\partial v}{\partial s} + \frac{w}{r} + \nu \frac{\partial u}{\partial x}\right) - \frac{1}{D}\left(N_x{}^o \frac{\partial^2 w}{\partial x^2} + N_s{}^o \frac{\partial^2 w}{\partial s^2}\right) = 0 \ ,$$

where

$$\nabla^4 \equiv \frac{\partial^4}{\partial s^4} + 2 \frac{\partial^4}{\partial s^2 \partial x^2} + \frac{\partial^4}{\partial x^4} \ .$$

We will consider cylindrical panels simply supported at the curved edges and with arbitrary support conditions on the straight edges. Given these boundary conditions and the fact that the curvature may be readily expressed in terms of a power series it is appropriate to choose the following set of displacement expressions:

$$v = \sum_{m=1}^{\infty} \sum_{n=1}^{\infty} V_{mn} \, \xi^{(n-1)} \sin m\pi\eta$$

$$u = \sum_{m=1}^{\infty} \sum_{n=1}^{\infty} U_{mn} \, \xi^{(n-1)} \cos m\pi\eta \qquad \text{(A.33)}$$

$$w = \sum_{m=1}^{\infty} \sum_{n=1}^{\infty} W_{mn} \, \xi^{(n-1)} \sin m\pi\eta$$

where η is the nondimensional longitudinal coordinate

$$\eta = \frac{X}{L} \tag{A.34}$$

and ξ is the nondimensional transverse coordinate

$$\xi = \frac{s}{\ell} \quad . \tag{A.35}$$

Also, ℓ is the transverse width measured along the curved middle surface, L is the axial length of the panel, and m is the number of axial half waves. These displacement expressions may be substituted into equations (A-32) to give recurrence relations between the various undetermined coefficients.

First we nondimensionalize equations (A.32) using equations (A-34) and (A-35) and the following dimensionless curvature expression:

$$\frac{1}{\rho} \equiv \frac{\ell}{r} = \sum_{i=1}^{k} a_i \, \xi^{(i-1)} \quad . \tag{A.36}$$

These steps result in the following equations:

$$\frac{\ell}{L} u_{\eta\eta} + \frac{1-\nu}{2} \cdot \frac{L}{\ell} u_{\xi\xi} + \frac{1+\nu}{2} v_{\eta\xi} + \nu \frac{w_{\eta}}{\rho} = 0$$

$$\frac{1}{\ell^2} \cdot \frac{\partial^2 v}{\partial \xi^2} + \frac{1-\nu}{2L^2} \cdot \frac{\partial^2 v}{\partial \eta^2} + \frac{1+\nu}{2\ell L} \cdot \frac{\partial^2 u}{\partial \xi \partial \eta} + \frac{\partial}{\partial \xi}\left(\frac{w}{\rho \ell^2}\right) = 0$$

$$\frac{h^2}{12} \bar{\nabla}^4 w + \frac{1}{\rho \ell}\left(\frac{1}{\ell} \cdot \frac{\partial v}{\partial \xi} + \frac{\nu}{L} \frac{\partial u}{\partial \eta} + \frac{1}{\rho \ell} w\right) - \tag{A.37}$$

$$- \frac{1}{D}\left(\frac{N_x^{\,o}}{L^2} \cdot \frac{\partial^2 w}{\partial \eta^2} + \frac{N_s^{\,o}}{\ell^2} \cdot \frac{\partial^2 w}{\partial \xi^2}\right) = 0$$

where

$$\bar{\nabla}^4 = \frac{1}{\ell^4} \cdot \frac{\partial^4}{\partial \xi^4} + \frac{2}{L^2 \ell^2} \cdot \frac{\partial^4}{\partial \xi^2 \partial \eta^2} + \frac{1}{L^4} \cdot \frac{\partial^4}{\partial \eta^4} \cdot$$

Substitution of the o displacement expressions gives:

$$\sum_{m=1}^{\infty}\sum_{n=1}^{\infty}\Bigg[-\frac{\ell}{L}m^2\pi^2 U_{mn}\xi^{(n-1)}+\frac{1-\nu}{2}\cdot\frac{L}{\ell}(n-1)(n-2)U_{mn}\xi^{(n-3)}+$$

$$+\frac{1+\nu}{2}m\pi(n-1)V_{mn}\xi^{(n-2)}+$$

$$+\nu\sum_{i=1}^{k}a_i\xi^{(i-1)}m\pi W_{mn}\xi^{(n-1)}\Bigg]\sin m\pi\eta=0$$

$$\sum_{m=1}^{\infty}\sum_{n=1}^{\infty}\Bigg[\frac{(n-1)(n-2)}{\ell^2}V_{mn}\xi^{(n-3)}-\frac{1-\nu}{2}\cdot\frac{m^2\pi^2}{L^2}V_{mn}\xi^{(n-1)}-$$

$$-\frac{1+\nu}{2}(n-1)\frac{m\pi}{\ell L}U_{mn}\xi^{(n-2)}+$$

$$+\frac{1}{\ell^2}\cdot\frac{\partial}{\partial\xi}\left(\sum_{i=1}^{k}a_i\xi^{(i-1)},W_{mn}\xi^{(n-1)}\right)\Bigg]\sin m\pi\eta=0 \qquad (A.38)$$

$$\sum_{m=1}^{\infty}\sum_{n=1}^{\infty}\Bigg[\Bigg(\frac{m^4\pi^2}{L^4}W_{mn}\xi^{(n-1)}-2\frac{m^2\pi^2}{L\ell}(n-1)(n-2)W_{mn}\xi^{(n-3)}+$$

$$+(n-1)(n-2)(n-3)(n-4)W_{mn}\xi^{(n-5)}\Bigg)+$$

$$+\frac{1}{\ell}\sum_{i=1}^{k}a_i\xi^{(i-1)}\frac{12}{h^2}\Bigg(\frac{1}{\ell}(n-1)V_{mn}\xi^{(n-2)}-$$

$$-\nu\frac{m\pi}{L}U_{mn}\xi^{(n-1)}+\frac{1}{\ell}\sum_{j=1}^{k}a_j\xi^{(j-1)}W_{mn}\xi^{(n-1)}\Bigg)+$$

$$+\Bigg(\frac{N_x^{o}\pi^2m^2}{DL^2}W_{mn}\xi^{(n-1)}-$$

$$-(n-1)(n-2)\frac{N_s^{o}}{D\ell^2}W_{mn}\xi^{(n-3)}\Bigg)\Bigg]\sin m\pi\eta=0\ .$$

When the exponential powers of ξ are adjusted to $(n-1)$, and account is taken of the linear independence of the terms of the double series, these recurrence relations result:

$$
\begin{aligned}
&- \alpha_m^{\,2} U_{mn} + \frac{1-\nu}{2} n(n+1)\, U_{m,n+2} + \frac{1+\nu}{2}\, \alpha_m^{\,n}\, V_{m,n+1} + \\
&\qquad + \nu \alpha_m \sum_{i=1}^{k} a_i \delta_{n,i}\, W_{m,n-i+1} = 0 \\
&n(n+1)\, V_{m,n+2} - \alpha_m^{\,2} \frac{1-\nu}{2}\, V_{mn} - \frac{1+\nu}{2}\, \alpha_m^{\,n}\, U_{m,n+1} + \\
&\qquad + \sum_{i=1}^{k} a_i\, n\, \delta_{n,i-1}\, W_{m,n-i+2} = 0 \\
&\left(\alpha_m^{\,2} + \frac{N_x {}^{o}\ell^2}{D} \right) \frac{\alpha_m^{\,2}}{N_4}\, W_{mn} - \left(\frac{n(n+1) N_s {}^{o}\ell^2}{D} + \frac{2\alpha_m^{\,2}}{N_2} \right) W_{m,n+2} + \\
&\qquad + W_{m,n+4} + \frac{12\ell^2}{N_4 h^2} \left(\sum_{i=1}^{k} a_i (n-i+1) \delta_{n,i-1}\, V_{m,n-i+2} - \right. \\
&\qquad - \nu \alpha_m \sum_{i=1}^{k} a_i\, \delta_{n,i}\, U_{m,n-i+1} + \\
&\qquad \left. + \sum_{i=1}^{k} \sum_{j=1}^{k} a_i\, a_j\, \delta_{n,i+j-1}\, W_{m,n-i-j+2} \right) = 0 \,.
\end{aligned}
\tag{A.39}
$$

In the above,

$$\alpha_m = \frac{m\pi\ell}{L}$$

$$\delta_{n,j} = \begin{cases} 0 \,, & n < j \\ 1 \,, & n \geq j \end{cases}$$

$$N_1 = n + 3$$

$$N_2 = (n+3)(n+2)$$

$$N_3 = (n+3)(n+2)(n+1)$$

$$N_4 = (n+3)(n+2)(n+1)n$$

N_x^o is the membrane stress due to axial load, positive for tension, and N_s^o is the stress due to pressure loading, positive for internal pressure.

The boundary conditions may be expressed, using equations (A.31 and A.33). Three sets of boundary conditions which satisfy equations (A.31) along the straight edges were considered:

a. Simply supported (SS3 in the notation of Ref. 4):

$$N_s = 0 : \sum_{n=1}^{\infty} \sum_{n=1}^{\infty} (nV_{m,n+1} - \nu\alpha_m U_{mn} + \sum_{i=1}^{k} a_i \delta_{n,i} W_{m,n-i+1}) \xi^{(n-1)} \cos m\pi\eta = 0$$

$$\delta u = 0 : \sum_{m=1}^{\infty} \sum_{n=1}^{\infty} U_{mn} \xi^{(n-1)} \cos m\pi\eta = 0$$

$$\delta w = 0 : \sum_{m=1}^{\infty} \sum_{n=1}^{\infty} W_{mn} \xi^{(n-1)} \sin m\pi\eta = 0$$

$$M_s = 0 : \sum_{m=1}^{\infty} \sum_{n=1}^{\infty} [n(n+1)W_{m,n+2} - \nu\alpha_m^2 W_{mn}] \xi^{(n-1)} \sin m\pi\eta = 0.$$

b. Simply supported with motion restricted in the transverse direction (SS4 in the notation of Ref. 4):

$$\delta v = 0 : \sum_{m=1}^{\infty} \sum_{n=1}^{\infty} V_{mn}\, \xi^{(n-1)} \sin m\pi\eta = 0$$

$$\delta u = 0 : \sum_{m=1}^{\infty} \sum_{n=1}^{\infty} U_{mn}\, \xi^{(n-1)} \cos m\pi\eta = 0$$

$$\delta w = 0 : \sum_{m=1}^{\infty} \sum_{n=1}^{\infty} W_{mn}\, \xi^{(n-1)} \sin m\pi\eta = 0$$

$$M_s = 0 : \sum_{m=1}^{\infty} \sum_{n=1}^{\infty} [n(n+1)W_{m,n+2} - \nu\alpha_m{}^2\, W_{mn}]\xi^{(n-1)} \sin m\pi\eta = 0.$$

c. Free edges:

$$N_s = 0 : \sum_{m=1}^{\infty} \sum_{n=1}^{\infty} [nV_{m,n+1} - \nu\alpha_m U_{mn} + \sum_{i=1}^{k} a_i \delta_{n,i} W_{n-i+1}]$$
$$\xi^{(n-1)} \cos m\pi\eta = 0$$

$$N_{sx} = 0 : \sum_{m=1}^{\infty} \sum_{n=1}^{\infty} [\alpha_m V_{mn} + nU_{m,n+1}]\xi^{(n-1)} \sin m\pi\eta = 0$$

$$\frac{\partial M_s}{\partial s} + 2\frac{\partial M_{xs}}{\partial s} = 0 : \sum_{m=1}^{\infty} \sum_{n=1}^{\infty} [n\alpha_m{}^2(2-\nu)W_{m,n+1} -$$
$$- n(n+1)(n+2)W_{m,n+3}]\xi^{(n-1)} \sin m\pi\eta = 0$$

$$M_s = 0 : \sum_{m=1}^{\infty} \sum_{n=1}^{\infty} [n(n+1)W_{m,n+2} - \nu\alpha_m{}^2 W_{mn}]\xi^{(n-1)} \sin m\pi\eta = 0.$$

APPENDIX B

COMPUTER PROGRAM

```
0000000001111111112222222223333333334444444445555555556666666666777777777 8
1234567890123456789012345678901234567890123456789012345678901234567890123456789 0
CARD
0001  C     OKLAHOMA STATE UNIVERSITY                    JACK W. VETTER
0002  C
0003  C     BUCKLING UNDER COMBINED LOADING OF CYLINDRICAL PANELS
0004  C     WRITTEN IN FORTRAN IV AND MAKING USE OF THE SSP SUBROUTINE PACKAGE
0005  C
0006  C     THIKRA = RATIO OF WIDTH TO THICKNESS OF THE PANEL
0007  C     ASPECT = RATIO OF WIDTH TO AXIAL LENGTH
0008  C     STEP   = INCREMENT IN BUCKLING PARAMETER VALUE
0009  C     FUDGE  = DIVISOR USED TO AVOID OVERFLOW OR UNDERFLOW
0010  C     EPSI   = ITERATION DIFFERENCE TEST FACTOR
0011  C     M      = NUMBER OF AXIAL HALF WAVES
0012  C     N      = NUMBER OF DISPLACEMENT SERIES TERMS
0013  C     KAY    = NUMBER OF TERMS IN THE CURVATURE SERIES
0014  C     PRESSR = CRITICAL PRESSURE BUCKLING PARAMETER
0015  C     START  = INITIAL VALUE FOR AXIAL LOAD PARAMETER
0016  C     FINISH = FINAL VALUE FOR BUCKLING LOAD PARAMETER
0017  C
0018        ODIMENSION DET(80,80),WORKER(80,80),LING(80),MING(80),AAAA(79,79),     N=24
0019       1BBBB(79),CCCC(79),SHAPE(80),STACK(19),DISPLT(11)                      N=24
0020       2 FORMAT(6E20.8)                                                       004
0021       3 FORMAT (2F10.5,E15.8,2F5.2,I1,2I2,3F10.5)
0022       6 FORMAT(16X,4HBETA,16X,4HFDET)                                        006
0023       7 FORMAT(16X,4HBETA,16X,4HFDET,16X,4HSTEP,16X,4HEPSI,15X,5HTEMP3)      007
0024       8 FORMAT(15X,5HZAMBA)                                                  008
0025       9 FORMAT (/15X,5HTEMP5,16X,4HFDET)                                     009
0026      12 FORMAT(/36H HERE ARE THE VALUES OF U AND ZARKOV/)                     011
0027      13 FORMAT(/36H HERE ARE THE VALUES OF V AND ZARKOV/)                     012
0028      14 FORMAT(/36H HERE ARE THE VALUES OF W AND ZARKOV/)                     013
0029      15 FORMAT (/8H DISPLT(,F4.1,5H ) = ,1PE16.4,10H      N =  ,0PF3.1/)     014
0030      17OFORMAT(/7X,7H THIKRA,13X,6HASPECT,15X,4HSTEP,13X,5HFUDGE,6X,4HEPSI
0031        1,1X,1HM,2X,1HN,1X,3HKAY,6X,6HPRESSR,9X,5HSTART, 8X,6HFINISH/)
0032      19 FORMAT  (1H ,10H  NUMBER= ,I2,8H  STACK(,I2,3H)= ,F10.5)             017
0033      200FORMAT (1PE20.8,E20.8,E20.8,0PF10.2,F10.2,I2,2I3,3F14.3)
0034         READ(5,3) THIKRA,ASPECT,STEP,FUDGE,EPSI,M,N,KAY,PRESSR,START,
0035        1FINISH
0036         WRITE(6,17)                                                          046
0037         WRITE(6,20) THIKRA,ASPECT,STEP,FUDGE,EPSI,M,N,KAY,PRESSR,START,
0038        1FINISH
0039         DO 10 I = 1,KAY                                                      048
0040         READ(5,3) STACK(I)                                                   049
0041      10 WRITE (6,19) I,I,STACK(I)                                            050
0042         ANEW = 0.3                                                          051
0043         PI = 3.1415927
0044         EM = M                                                              054
0045         MAX = N + 1
0046         MAXA = N+ 2                                                         056
0047         NPTHRE = N + 3                                                      057
0048         MAXB = N + 4                                                        058
0049         MAXC = 2*N + 4                                                      059
0050         MI = 2 *N  + 5                                                      060
0051         ME = 2*N + 6                                                        061
0052         MU = 2*N +7                                                         062
0053         MY = 2*N + 9
0054         MO = 3*N + 6
0055         MA = 3*N + 7                                                        063
```

```
      0000000001111111111222222222233333333334444444444555555555566666666667777777778
      1234567890123456789012345678901234567890123456789012345678901234567890123456789
CARD
0056        J = 3*N+ 8                                                          064
0057        ZAMBA = 0.0                                                         065
0058        ALFA = EM*PI*ASPECT                                                 066
0059        DO 100 L =1,J                                                       072
0060        DO 100 K = 1,J                                                      077
0061      100 DET(L,K) = 0.0                                                    078
0062  C     CALCULATE THE BOUNDARY CONDITIONS AND THEN SUBSTITUTE               083
0063        DET (N+1,1) = 1.0
0064        DO 101 K = 1,MAXA
0065      101 DET(MAXA,K) = 1.0
0066         .DET(NPTHRE,NPTHRE) = 1.0
0067        DO 102 K = 1,MAXA
0068      102 DET(MAXB,MAXA + K ) = 1.0
0069        DET(MI,MI) = 1.0
0070        DO 103 K = MI,J
0071      103 DET(ME,K) = 1.0
0072        DET(MU,MU) = 2.0
0073        TEMPO = 0.0
0074        DO 104 K = MU,J
0075        TEMPO = TEMPO + 1.0
0076        TAMPA = TEMPO + 1.0
0077      104 DET(2*N+8,K) = TEMPO*TAMPA
0078  C
0079        FDET = 0.0                                                          116
0080        PRESSR = PRESSR*PI*PI/16.
0081        BETA = START                                                        115
0082        GAMMA = ALFA*ALFA + BETA                                            117
0083        DO 200 K = 1,N                                                      104
0084        AN = K                                                              105
0085        DET(K,K) = -ALFA*ALFA                                               106
0086        DET(K,K+2) = ((1.0 - ANEW)/2.0)*AN*(AN + 1.0)                       107
0087        DET(K,N+3+K) = ((1.0+ANEW)/2.0)*ALFA*AN                             108
0088        DET(K+MAXB,N+2+K) = -((1.0-ANEW)/2.0)*ALFA*ALFA                     109
0089        DET(K+N+4,K+N+4) = AN*(AN+1.0)                                      110
0090        DET(K+4+N,K+1) = -((1.0+ANEW)/2.0)*ALFA*AN                          112
0091        DET(K+8+N+N,K+N+N+8) = 1.0                                          113
0092        DET(K+8+N+N,K+N+N+6) = (PRESSR-2.*ALFA*ALFA)/((AN+2.)*(AN+3.))
0093      200DET(K+8+N+N,K+N+N+4)=ALFA*ALFA*GAMMA/(AN*(AN+1.)*(AN+2.)*(AN+3.))
0094  C     THE FOLLOWING TERMS ARE FOR CYLINDRICAL EFFECTS, DUE TO CURVATURE   123
0095        DO 206 L = 1,N                                                      129
0096        ENN = L                                                             146
0097        EN4 = ENN*(ENN+1.)*(ENN+2.)*(ENN+3.)
0098        DO 204 K = 1,KAY
0099        IF(L - K) 204,203,203                                               126
0100      203 DET(L,N+N+4+L-K+1) = ANEW*ALFA*STACK(K)                           127
0101        DET(N+N+8+L,L-K+1)= -12.*THIKRA*THIKRA*ALFA*ANEW*STACK(K)/EN4
0102      204 CONTINUE                                                          128
0103        DO 206 K = 1,KAY
0104        IF(L-K+1)  206,205,205                                              132
0105      205 DET(N+4+L,N+N+4+L-K+2) = ENN*STACK(K)                             134
0106        EYE = K                                                             140
0107        DET(N+N+8+L,N+2+L-K+2)=12.*THIKRA*THIKRA*STACK(K)*(ENN-EYE+1.)/EN4
0108      206 CONTINUE                                                          135
0109        DO 216 L = 1,N                                                      152
0110        DO 216 K1 = 1,KAY                                                   155
```

```
     00000000011111111112222222222333333333344444444445555555556666666666777777777 8
     12345678901234567890123456789012345678901234567890123456789012345678901234567890
CARD
0111       DO 216 K2 = 1,KAY                                                      156
0112       IF (L-K1-K2+1)  216,249,249                                            157
0113    2490DET(N+N+8+L,N+N+4+L-K1-K2+2) =   DET(N+N+8+L,N+N+4+L-K1-K2+2) +       158
0114      1((12.*THIKRA*THIKRA*STACK(K1)*STACK(K2))/(L*(L+1)*(L+2)*(L+3))
0115    216 CONTINUE                                                             160
0116       DO 302 L = 1,J                                                        162
0117       DO 302 K = 1,J                                                        163
0118    302 WORKER(K,L) = DET(K,L)/FUDGE
0119       WRITE(6,6)                                                            165
0120       CALL MINV(WORKER,J,FDET,LING,MING)                                    166
0121       FACTOR = ABS(FDET/1000.0)                                             167
0122  C                                                                          168
0123    399 TEMP1 = FDET                                                         169
0124  C                                                                          170
0125       TEMP2 = BETA                                                          171
0126       WRITE(6,2)      BETA,FDET                                             172
0127       BETA = BETA + STEP                                                    173
0128       IF(FINISH  - BETA)304,304,950
0129    304 GAMMA = ALFA*ALFA + BETA
0130       DO 850 K = MY,J
0131       DO 850 L = MI,J
0132    850 DET(K,L) = 0.0
0133       DO 305 K = 1,N                                                        175
0134       AN = K                                                                176
0135       DET(K+8+N+N,K+N+N+8) = 1.0
0136       DET(K+8+N+N,K+N+N+6) = (PRESSR-2.*ALFA*ALFA)/((AN+2.)*(AN+3.))
0137    305 DET(K+8+N+N,K+N+N+4)=ALFA*ALFA*GAMMA/(AN*(AN+1.)*(AN+2.)*(AN+3.))
0138       DO 316 L = 1,N                                                        179
0139       DO 316 K1 = 1,KAY                                                     182
0140       DO 316 K2 = 1,KAY                                                     183
0141       IF (L-K1-K2+1) 316,349,349                                            184
0142    3490DET   (N+N+8+L,N+N+4+L-K1-K2+2) = DET (N+N+8+L,N+N+4+L-K1-K2+2) +    185
0143      1((12.*THIKRA*THIKRA*STACK(K1)*STACK(K2))/(L*(L+1)*(L+2)*(L+3))
0144    316 CONTINUE                                                             187
0145       DO 402 L = 1,J                                                        188
0146       DO 402 K = 1,J                                                        189
0147    402 WORKER(K,L) = DET(K,L)/FUDGE                                         190
0148       CALL MINV(WORKER,J,FDET,LING,MING)                                    192
0149       FDET = FDET/FACTOR                                                    193
0150  C                                                                          194
0151       IF (TEMP1) 420,421,421                                                195
0152    420 IF(FDET)  399,399,500                                                196
0153    421 IF(FDET) 500,399,399                                                 197
0154  C                                                                          198
0155  C     DONE STEPPING, NOW JUST USE NEWTON'S METHOD AND ITERATE               199
0156    500 TEMP5 = TEMP2                                                        200
0157       TEMP3 = BETA                                                          201
0158       TEMP4 = TEMP1                                                         202
0159       WRITE(6,6)                                                            203
0160       WRITE(6,2) BETA,FDET                                                  204
0161    405 BETA = (FDET*TEMP5 - TEMP4*TEMP3)/(FDET - TEMP4)
0162       IF(ABS((BETA-TEMP3)/STEP)-EPSI)  600,600,403                          236
0163    403 TEMP5 = TEMP3                                                        206
0164       TEMP3 = BETA                                                          207
0165       TEMP4 = FDET                                                          208
```

```
     00000000011111111112222222222333333333344444444445555555556666666666777777777778
     12345678901234567890123456789012345678901234567890123456789012345678901234567890
CARD
0166       GAMMA = ALFA*ALFA + BETA                                                209
0167       DO 851 K = MY,J
0168       DO 851 L = MI,J
0169   851 DET(K,L) = 0.0
0170       DO 406 K = 1,N
0171       AN = K                                                                  211
0172       DET(K+8+N+N,K+N+N+8) = 1.0
0173       DET(K+8+N+N,K+N+N+6) = (PRESSR-2.*ALFA*ALFA)/((AN+2.)*(AN+3.))
0174   406 DET(K+8+N+N,K+N+N+4)=ALFA*ALFA*GAMMA/(AN*(AN+1.)*(AN+2.)*(AN+3.))
0175       DO 416 L = 1,N                                                          214
0176       DO 416 K1 = 1,KAY                                                       217
0177       DO 416 K2 = 1,KAY                                                       218
0178       IF (L-K1-K2+1) 416,449,449                                              219
0179   4490DET   (N+N+8+L,N+N+4+L-K1-K2+2) = DET (N+N+8+L,N+N+4+L-K1-K2+2) +      220
0180      1((12.*THIKRA*THIKRA*STACK(K1)*STACK(K2))/(L*(L+1)*(L+2)*(L+3))
0181   416 CONTINUE                                                               222
0182  C                                                                           223
0183       WRITE(6,9)                                                             224
0184       WRITE (6,2) TEMP5,FDET
0185       DO 404 L = 1,J                                                         226
0186       DO 404 K = 1,J                                                         227
0187   404 WORKER(K,L) = DET(K,L)/FUDGE                                           228
0188       ZAMBA = ZAMBA + 1.0                                                    229
0189       CALL MINV(WORKER,J,FDET,LING,MING)                                     231
0190       FDET = FDET/FACTOR                                                     232
0191       GO TO 405                                                              205
0192  C                                                                           234
0193   600 WRITE(6,7)                                                             38
0194       WRITE(6,2) BETA,FDET,STEP,EPSI,TEMP3
0195       TEMP = BETA*2.0/(THIKRA*PI*SQRT(48.*(1.-ANEW*ANEW)))
0196       TEMP = BETA*16./(PI*PI)
0197       WRITE(6,2) TEMP,FDET
0198   604 WRITE (6,8)                                                            249
0199       WRITE(6,2) ZAMBA                                                       250
0200       GAMMA = ALFA*ALFA + BETA
0201       DO 852 K = MY,J
0202       DO 852 L  = MI,J
0203   852 DET(K,L) = 0.0
0204   407 DO 408 K = 1,N                                                         253
0205       AN = K                                                                 254
0206       DET(K+8+N+N,K+N+N+8) = 1.0
0207       DET(K+8+N+N,K+N+N+6) = (PRESSR-2.*ALFA*ALFA)/((AN+2.)*(AN+3.))
0208   408 DET(K+8+N+N,K+N+N+4)=ALFA*ALFA*GAMMA/(AN*(AN+1.)*(AN+2.)*(AN+3.))
0209       DO 516 L = 1,N                                                         257
0210       DO 516 K1 = 1,KAY                                                      260
0211       DO 516 K2 = 1,KAY                                                      261
0212       IF (L-K1-K2+1)  516,549,549                                            262
0213   5490DET   (N+N+8+L,N+N+4+L-K1-K2+2) = DET (N+N+8+L,N+N+4+L-K1-K2+2) +     263
0214      1((12.*THIKRA*THIKRA*STACK(K1)*STACK(K2))/(L*(L+1)*(L+2)*(L+3))
0215   516 CONTINUE                                                               265
0216       DO 707 K = 1,MAXC
0217       BBBB(K) = - DET(K,MI)/FUDGE
0218       DO 707 L = 1,MAXC
0219   707 AAAA(K,L) = DET(K,L) / FUDGE
0220       DO 709 K = 1,NPTHRE
```

```
     00000000011111111112222222222333333333344444444445555555556666666666777777777 8
     12345678901234567890123456789012345678901234567890123456789012345678901234567890
CARD
0221         DO 709 L = 1,MAXC
0222         AAAA(K+MAXC,L) = DET(MI+K,L)/FUDGE
0223       709 AAAA(L,MAXC+K) = DET(L,MI+K)/FUDGE
0224         DO 713 K = 1,NPTHRE
0225         BBBB(MAXC+K) = - DET(MI+K,MI)/FUDGE
0226         DO 713 L = 1,NPTHRE
0227       713 AAAA(MAXC+K,MAXC+L) = DET(MI+K,MI+L)/FUDGE
0228         CALL MINV (AAAA,MA,FDET,LING,MING)                              273
0229         CALL GMPRD (AAAA,BBBB,CCCC,MA,MA,1)                             274
0230         DO 710 K = 1,MAXC
0231       710 SHAPE(K) = CCCC(K)
0232         SHAPE(MI) = 1.0
0233         DO 714 K = MI,MA
0234       714 SHAPE(K+1) = CCCC(K)
0235         CALL MXOUT (4,SHAPE,J,1,0,60,132,1)                             279
0236   C     WE NOW SOLVE FOR THE U-DISPLACEMENT                             283
0237         ZARKOV = - 0.1                                                  285
0238         WRITE (6,12)                                                    286
0239         DO 900 IPY = 1,11                                               287
0240         TERM = 0.0                                                      288
0241         ZARKOV = ZARKOV + 0.1                                           289
0242         DO 800 K = 1,MAXA                                               290
0243         TERM =  SHAPE(K)*(ZARKOV**( K - 1 )) + TERM
0244       800 WRITE (6,2) TERM,ZARKOV,EM                                    292
0245       900 DISPLT(IPY) = TERM                                            293
0246         CALL RATIO(DISPLT)                                              294
0247         DO 901 IPY = 1,11                                               295
0248         ZARKOV = IPY - 1                                                296
0249       901 WRITE(6,15) ZARKOV,DISPLT(IPY),EM                             297
0250   C     NOW FOR THE V-DISPLACEMENTS                                     299
0251         ZARKOV = - 0.1                                                  301
0252         WRITE (6,13)                                                    302
0253         DO 930 IPY = 1,11                                               303
0254         TERM = 0.0                                                      304
0255         ZARKOV = ZARKOV + 0.1                                           305
0256         DO 931 K = NPTHRE,MAXC                                          306
0257         TERM = TERM +  SHAPE(K)*(ZARKOV**(K - 1 - MAXA))                307
0258       931 WRITE (6,2) TERM,ZARKOV,EM                                    308
0259       930 DISPLT (IPY) = TERM                                           309
0260         CALL RATIO(DISPLT)                                              301
0261         DO 932 IPY = 1,11                                               311
0262         ZARKOV = IPY - 1                                                312
0263       932 WRITE (6,15) ZARKOV,DISPLT(IPY), EM                           316
0264   C     NOW THE W - DISPLACEMENTS                                       315
0265         ZARKOV = - 0.1                                                  317
0266         WRITE (6,14)                                                    318
0267         DO 940 IPY = 1,11                                               319
0268         TERM = 0.0                                                      320
0269         ZARKOV = ZARKOV + 0.1                                           321
0270         DO 941 K = MI,J                                                 322
0271         TERM = TERM + SHAPE(K)*(ZARKOV**(K - 1 - MAXC))
0272       941 WRITE (6,2) TERM, ZARKOV, EM                                  324
0273       940 DISPLT  (IPY) = TERM                                          325
0274         CALL RATIO(DISPLT)                                              326
0275         DO 942 IPY = 1,11                                               327
```

```
     00000000011111111112222222222333333333344444444455555555566666666667777777778
     12345678901234567890123456789012345678901234567890123456789012345678901234567890
CARD
0276         ZARKOV = IPY - 1                                                    328
0277       942 WRITE (6,15) ZARKOV,DISPLT(IPY),EM                                329
0278       950 CONTINUE
0279         STOP                                                                330
0280         END                                                                 331
0281         SUBROUTINE RATIO(A)                                                 332
0282         DIMENSION A(11)                                                     333
0283         GLUNT = 0.0                                                         334
0284         DO 921 IPY = 1,11                                                   335
0285         IF(ABS(A(IPY)) - GLUNT) 921,921,920                                 336
0286       920 GLUNT = ABS(A(IPY))                                               337
0287       921 CONTINUE                                                          338
0288         DO 910 IPY = 1,11                                                   339
0289       910 A(IPY) = (A(IPY))/GLUNT                                           340
0290         RETURN                                                              341
0291         END                                                                 342
```

VITA

Jack William Vetter

Candidate for the Degree of

Doctor of Philosophy

Thesis: CLASSICAL BUCKLING OF CYLINDRICAL PANELS

Major Field: Engineering

Biographical:

Personal Data: Born November 20, 1938, in Kansas City, Missouri, the son of Mr. and Mrs. Robert Paul Vetter.

Education: Graduated from Shawnee-Mission High School, Merriam, Kansas, in May, 1956. Received the Degree of Bachelor of Science in Aeronautical Engineering from the University of Kansas in March, 1961, and the Degree of Master of Science in Engineering Mechanics from the University of Kansas in June, 1966. Completed requirements for the Degree of Doctor of Philosophy from Oklahoma State University in May, 1970.

Professional Experience: Peace Corps Volunteer in Ecuador, 1962-64. Mechanical Engineer at Naval Research Laboratory, Summers of 1966, 1967 and 1968. Graduate Teaching Assistant, Oklahoma State University, 1966-67, 1967-68; half-time Instructor, 1968-69.